N70-71942

NASA-CR-108009

Informal

Progress Report

"Flutter of Thermally Stressed Plates Subjected to Large Deflections"

NASA Grant Number NGL 36-008-109

Ohio State University

Research Foundation Project Number 2792

Period

1 July 1969 to 31 December 1969

Introduction

Overall progress during this period has been quite satisfactory. A few problems were encountered but they have not caused any serious delay. The graduate student who was employed on the experimental phase of the program received an offer of a position that he could not refuse. As a result he has left the Ohio State University causing a slowdown in the experimental work. Because of this, the effort to prepare a paper on stresses in the presence of mixed boundary conditions, which requires the experimental data, has been delayed and the task of beginning a parametric study of flutter with thermal stresses and mode coupling has been moved up. Rising costs coupled with the fixed resources of the Grant has forced the principle investigator to reduce his release time for the project to only six percent as of 1 October 1969.

The work to be accomplished for the period 1 July to 31 December was outlined in the Research Plan dated 29 August 1969. Briefly stated, it and the projected manpower were as follows:

a. Conduct a two phase experimental program to,

   1. Measure the thermal strains in the vicinity of the root of both a rectangular and a triangular cantilever plate and compare to analytical strains when the measured temperature is used in the calculations.

   2. Relate quantitatively the dynamic response to initial deformation.

   Manpower: one student, 1/2 time, 1 July-30 September
   1/4 time, 1 October-31 December

b. Conduct a parametric study of thermal buckling eigenvalues and vibration eigenvalues for symmetrical tapered plates of constant thickness.

Manpower: one student, 1/3 time, 1 July-30 September

c. Prepare a technical report on the stress analysis work of 1 April-30 June, based on the previous Progress Report, dated 29 July 1969.

Manpower: one student, 1/3 time, 1 October-31 December

d. Study the effect of variable thickness on the stress distribution in thermally stressed, symmetrically tapered plates.

Manpower: one student, 1/4 time, 1 October-31 December

The progress on each task follows:

a. <u>The Experimental Program</u>

1. Thermal Stress: Strains have been obtained for a rectangular plate that verifies the previously obtained analytical solution along the free edge of the plate. A one-quarter inch thick aluminum plate was clamped between two steel bars of 2" x 2" cross section. Although it is virtually impossible to achieve completely the condition of zero strain in the chordwise direction at the root, sufficient constraint did exist to verify the shape of the stress curve. The results of three separate tests are shown in Figure 1. The temperature distribution obtained in these steady state tests is shown in Figure 2. Other tests, not included herein, show that the root stresses vary, as expected, with heat soak time. As the steel bars heat, they expand and

relieve the root stresses. This occurs very slowly, however, so that steady state conditions can be assumed for any given reading. The location of thermocouples and strain gages is shown in Figures 3 and 4. Similar data are desired for a triangular plate.

2. Initial Deformation and Dynamic Response: Initial deformation and frequency data have been recorded for several plates. The minimum frequency in every instance has been observed to decrease as the initial deflection increases just as the theory predicts. The equations for quantitatively relating measured initial deflections to the measured frequency are shown in Appendix I. A major problem in this area is to obtain the temperature distribution from which the buckling eigenvalues may be calculated in the case of rapid heating. Steady state temperature recording is available but transient temperature measuring equation is not available in sufficient channels to properly define the temperature distribution. An indication of how important the temperature distribution may be is shown in Figures 5 and 6 from data obtained in AAE 710, the fifth year laboratory course. In Figure 5, both the torsion and bending frequencies are shown vs. ΔT with a plot of ΔT vs. time. ΔT is the difference between the temperatures at the plate edge and the plate center. It is

indicative of the thermal gradients but does not reflect the changing temperature distribution as heat is conducted through the plate. The plate was 16.67 inches in length with a 10" chord. In the post buckled region its deflected shape was observed to be as shown.

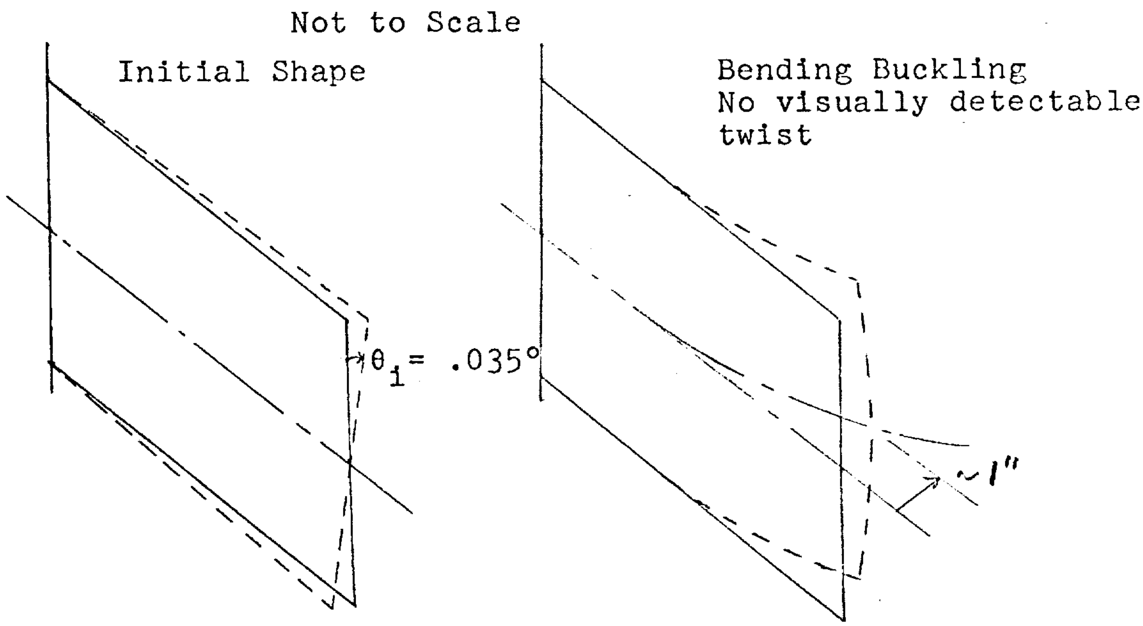

The bending frequency is seen to be very sensitive to the initial temperature distribution as indicated by the initial non-linearity of the $(\omega/\omega_o)^2_B$ curve; but when the large bending deflections occur as sketched, the bending frequency increases while the torsion frequency levels off. Note that the torsion response is not too sensitive to the changes occurring in temperature distribution as reflected by its relative linearity up to bending deformation.

In Figure 6 is presented the same information for the same plate except that 6.67 inches was carefully removed from the end, leaving a square plate, thus changing both the ω_{oB}/ω_{oT} and $\Delta T_B/\Delta T_T$ ratios. In the post buckled region, its deflected shape was observed to be as shown:

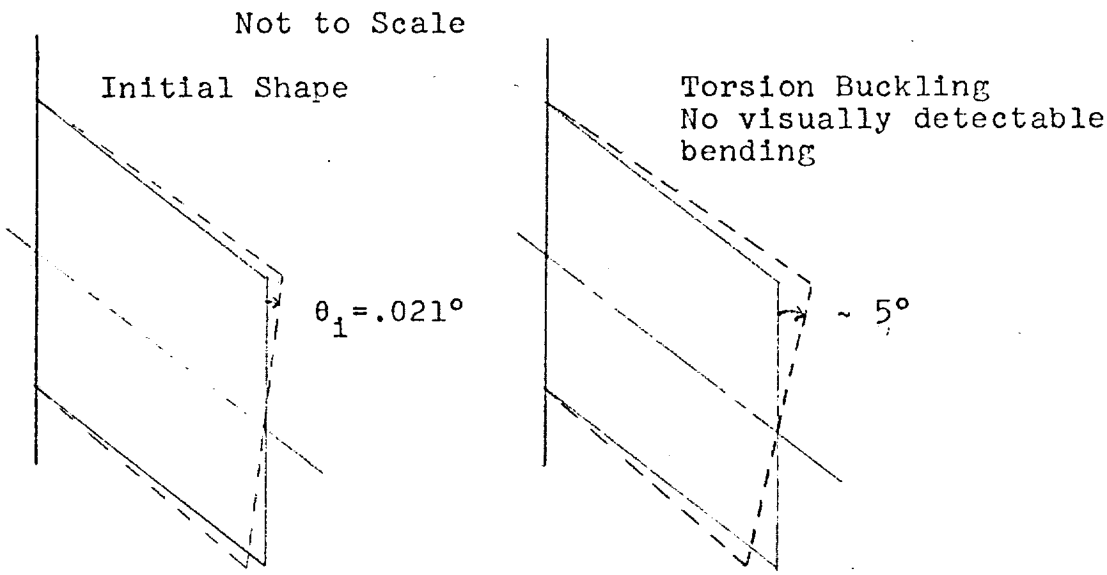

In Figure 6, the same sensitiveness of the bending mode and insensitiveness of the torsion mode to the temperature distribution will be noted. However, the torsion frequency will now be observed to increase, while the bending frequency levels off. This is as predicted by the coupled mode theory when $\Delta T_B/\Delta T_T$ increases. The bending mode response indicates that it may be necessary to calculate the buckling eigenvalues at each point in time when the temperature distribution has changed. If the buckling eigenvalues should be relatively insensitive to the temperature distribution, a considerable reduction in the calculations for flutter would result.

b. Parametric Study of Frequencies and Thermal Buckling Eigenvalues for Tapered Symmetrical Plates of Constant Thickness

This phase for nine term deflection functions and a sixteen term stress function has been completed. The results provide information about the bounds for frequency ratios and buckling eigenvalue ratios that are needed for the parametric study of flutter. The frequency data are presented in Table I. Plotting the frequency ratios indicates that, for a cantilever plate, the minimum value of ω_{oB}/ω_{oT} approaches unity as the plate aspect ratio approaches zero; i.e., the second mode frequency is never less than the first mode. This is contrary to our experience with cantilever beams where it is well known that the bending frequency may exceed the torsion frequency. The importance of the frequency ratio as an influence on the mode coupling is shown in Appendix II of the attached revised paper, "Modal Coupling in Thermally Stressed Plates". An error in subtraction in the original paper covered up the fact that mode coupling is affected by the frequency ratio as well as the buckling eigenvalue ratio. For plates of relatively large aspect ratio, i.e., greater than unity, the frequency ratio, ω_{oB}/ω_{oT}, is small and may be taken as zero. However, for small aspect ratios, ω_{oB}/ω_{oT} appears to approach unity and cannot be neglected. One set of parametric curves for all plates, for which the ratio of first mode thermal buckling to second mode thermal buckling is, $\Delta T_B/\Delta T_T = 1.1$, and the initial imperfection parameters are, $\psi_i = .1$, and $\phi_i = .02$, is shown in Figure 7. Note that the frequency ratio, which is a function of the planform shape, thickness distribution, material properties and boundary conditions, can have a marked effect on the post buckling behavior of plates. These effects have not been noticed in the laboratory because the plates tested to date have all had very small values of ω_{oB}/ω_{oT}. Further investigation, both analytically and experimentally, is indicated.

The thermal buckling eigenvalues are presented in Table II. Figure 8 shows a typical plot of the assumed temperature distribution used in the calculations. In all cases, the temperature was assumed such that the isotherms were parallel to the plate edges. Since the eigenvalues are functions of the temperature distribution, eigenvalues for other temperature distributions have been evaluated but are not included in this report. They indicate that, although the individual eigenvalues may change considerably, their ratio (the important parameter) does not vary appreciably as the form of the temperature surface changes. The temperature distributions investigated do not include any that would be similar to that existing in the initial part of rapid heating discussed under item a.2. At this time, it appears that the 9-term deflection function for symmetrical bending may not be sufficient to define the bending buckling mode for all aspect ratios and tapers. A 15-term solution was used in a few cases to assure that the 9-term solution is adequate. The 9-term solution for vibration had previously been favorably compared to both solutions in the literature as well as experimental data. The buckling eigenvalues obtained when 15-term deflection functions were used are shown for comparison to the 9-term answers:

	Terms	K_B	K_T	Γ_B/Γ_T
AR = .75, β = 1	9	45.989	41.049	1.1203
	15	45.368	40.973	1.1072
AR = 1.67, β = 1	9	558.04	501.4	1.113
	15	531.52	499.07	1.065
AR = 2.0, β = 1	9	1110.5	928.67	1.1958
	15	971.16	927.07	1.0476
β = .4	9	3024.5	2970.6	1.018
	15	71.157	2944.7	.02416
β = 0	9	4946.2	4953.0	.9986
	15	131.37	4900.4	.0268

The values shown indicate that the buckling eigenvalues are probably sufficiently close for $\beta = 1$ up to an aspect ratio of two. But as β decreases for an aspect ratio of two, the bending buckling eigenvalue decreases drastically. More work is to be done in this area. The difficulty may very well be two-fold: 1) the eigenvalue subroutine may be breaking down because the mid-plane energy matrix becomes ill-conditioned and/or 2) although observation of experimental buckling deformations shows that the torsion buckling mode does not differ appreciably from the torsion vibration mode, page 5, the bending buckling mode appears to differ considerably from the vibration bending mode in both the degree of chordwise deformation and in the degree of bending, page 4, thus requiring higher order terms in the assumed solution. It may be of interest to note the savings in computer time as a result of formal integration of the matrix elements. Using nine term deflection functions and a sixteen term stress function, the present program on the IBM 360 will produce nine symmetrical (bending) vibration modes and frequencies, nine symmetrical buckling modes and eigenvalues and nine antisymmetrical (torsion) vibration modes and frequencies and nine antisymmetrical buckling modes and eigenvalues in 1.2 minutes. For comparison, a similar program, using numerical integration, on the IBM 7094, to produce one bending vibration mode and frequency, one bending buckling mode and eigenvalue, one torsion vibration mode and frequency, and one torsion buckling mode and eigenvalue, requires 43.08 minutes.

c. Stress Analysis Report

The work scheduled for this task has been replaced by work noted below that was originally scheduled to begin 1 January 1970.

The parametric study of flutter in the presence of thermal stresses: The equations have been derived and a computer program written whereby regions of stability may be predicted for various combinations of parameters. The program has been 'debugged' and work on the parametric study has started. Further definition of the bounds of some of the parameters is needed to avoid making runs into physically impossible regions. It is expected that more detailed work and research into the linear problem may lead to a suitable definition of the parameter bounds. The equations and a sample of the results to date are given in Appendix II.

d. Effect of Variable Thickness on Stress Distribution

Problems have been encountered in the formal integration of the matrix elements for this work. The thickness function appears in the denominator of one integrand and although formal integration can be accomplished, it will save little computer time because of the many additional calculations that must be made; e.g., a linear thickness variation of the form, $t = ax + by + c$, would require an order of magnitude times as many calculations for each matrix element as is required for the constant thickness plate. In view of the fact that the matrix elements for both variable thickness and non-symmetrical planforms can be computed in the same time as that required for constant thickness plates of symmetrical planform by numerical integration, the numerical integration scheme becomes more than competitive for plates in general. A program for symmetrical plates of constant thickness has been written and successfully used with the IBM 7094 Computer to check the results of the IBM 360 program where formal integration was used. That program is presently being adapted to the IBM 360 where it is expected that each set of eigenvalues for either uniform or non-uniform plates will require about ten minutes of computer time. The program is now ready for a final check run. Once it is operational, it may also be applied directly to accomplish that part of the work scheduled for 1 January 1970 to 30 June 1970 pertaining to the thermal buckling and vibration eigenvalues of non-uniform plates.

Conclusion

Although operating costs have increased, considerably progress has been made during this report period, especially in view of the loss of one graduate student and the necessity for a reduction of participation time for the principal investigator.

A block diagram of the problem, showing the relationship of the different facets on which work is being accomplished, is shown in Figure 9. Each block represents an independent problem, once the inputs into the block are known. Thus parametric studies may be conducted at any point; but, when an explicit lifting surface structure and flight profile are specified, then the solution must proceed in an orderly fashion from temperature input to aeroelastic output.

All work to date has used an assumed temperature distribution or a temperature distribution obtained from experiments with radiant heat lamps. We still intend to prepare a report on the thermal stress distribution in cantilever plates but some additional work in this area is also required.

At present, the different facets of the problem are being attacked separately. Ultimately, it is expected that all of the computer programs will be unified into one single program to yield answers to both static and dynamic aeroelastic phenomena for any applicable set of inputs.

10 Dec 69

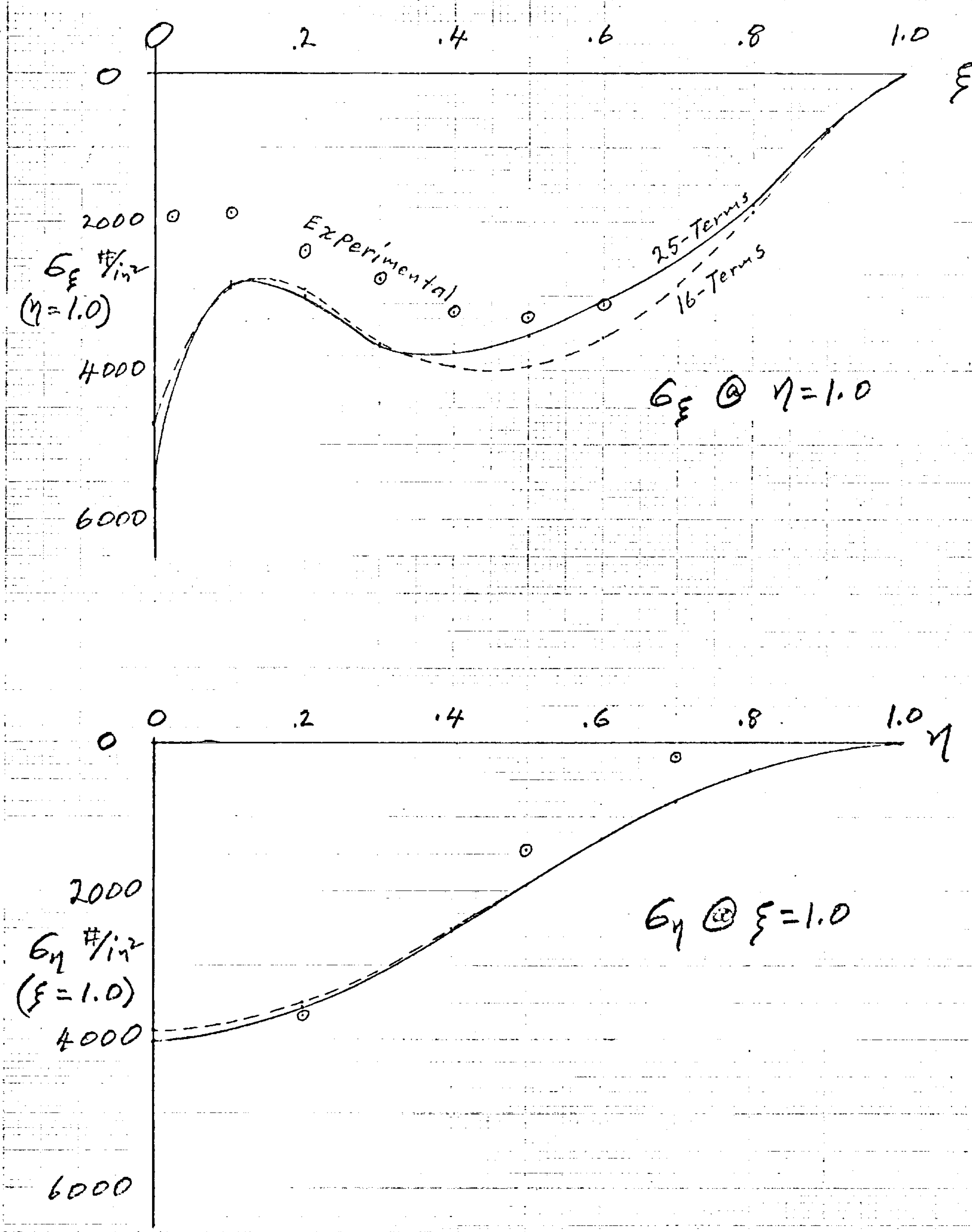

Edge Stresses, Cantilever plate, β=0

Fig. I

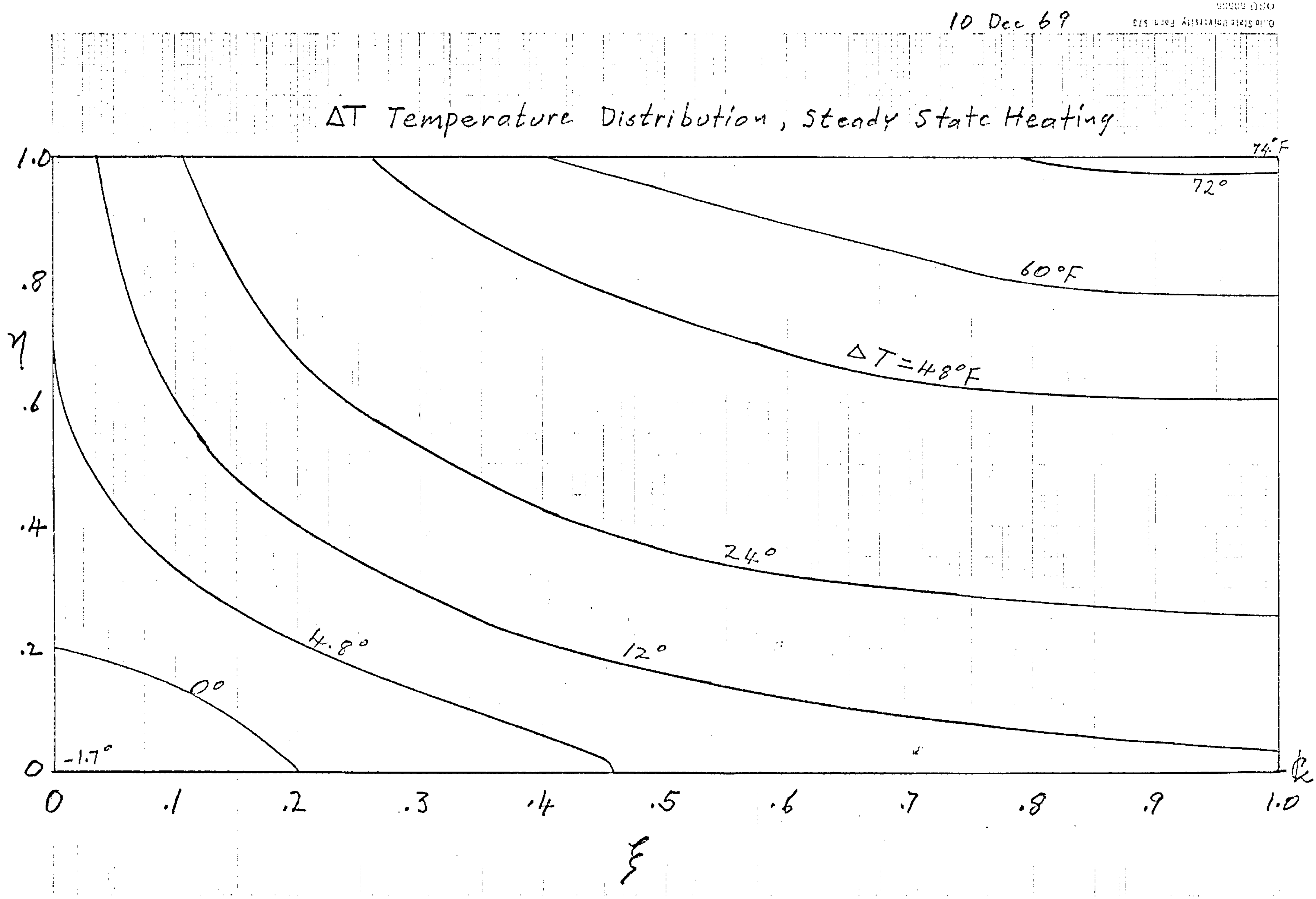
10 Dec 69
ΔT Temperature Distribution, Steady State Heating
74°F
72°
60°F
ΔT=48°F
24°
12°
4.8°
0°
-1.7°
1.0
.8
.6
.4
.2
0
η
0
.1
.2
.3
.4
.5
.6
.7
.8
.9
1.0
ξ

Fig. 2

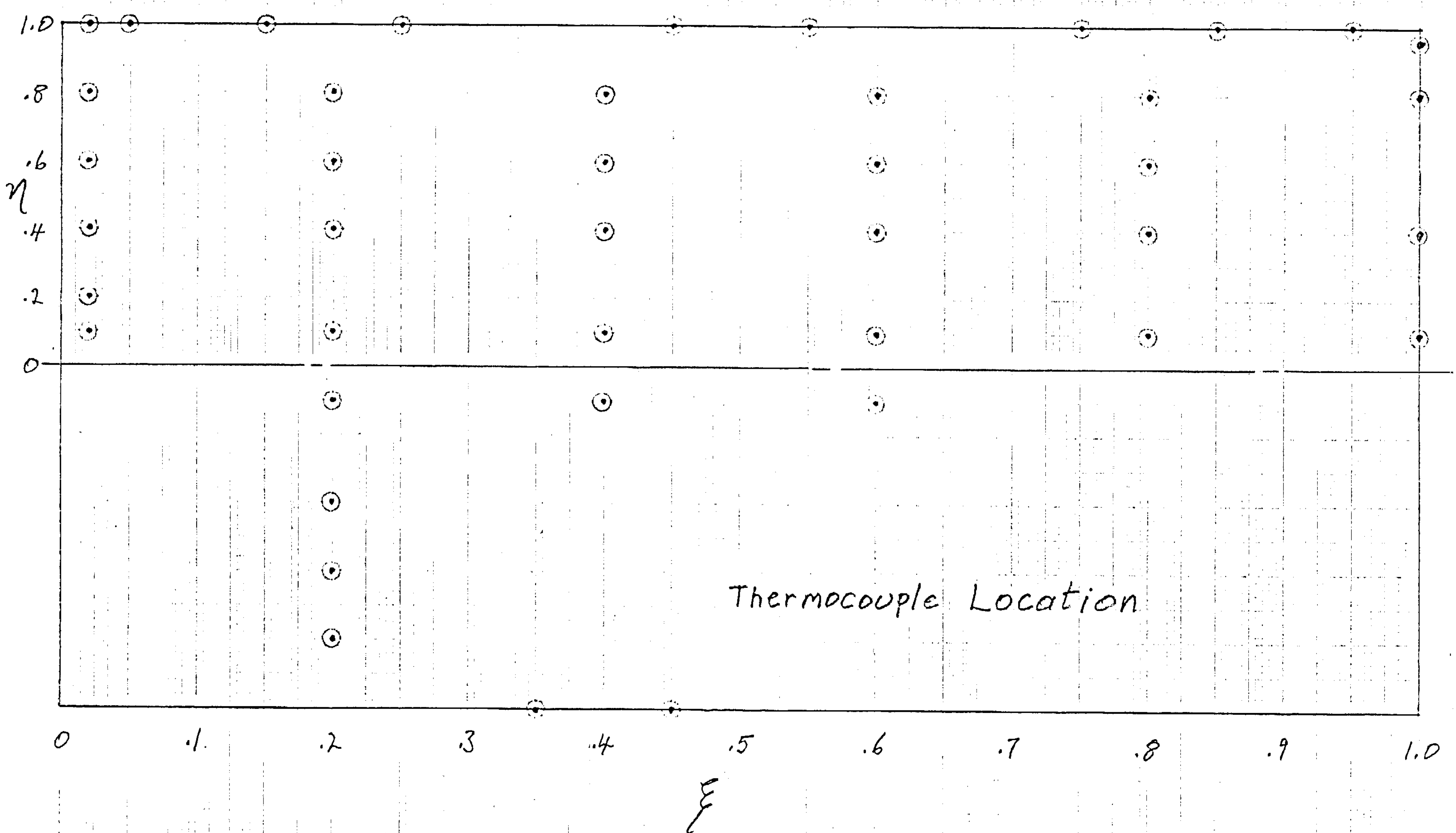

Fig. 3

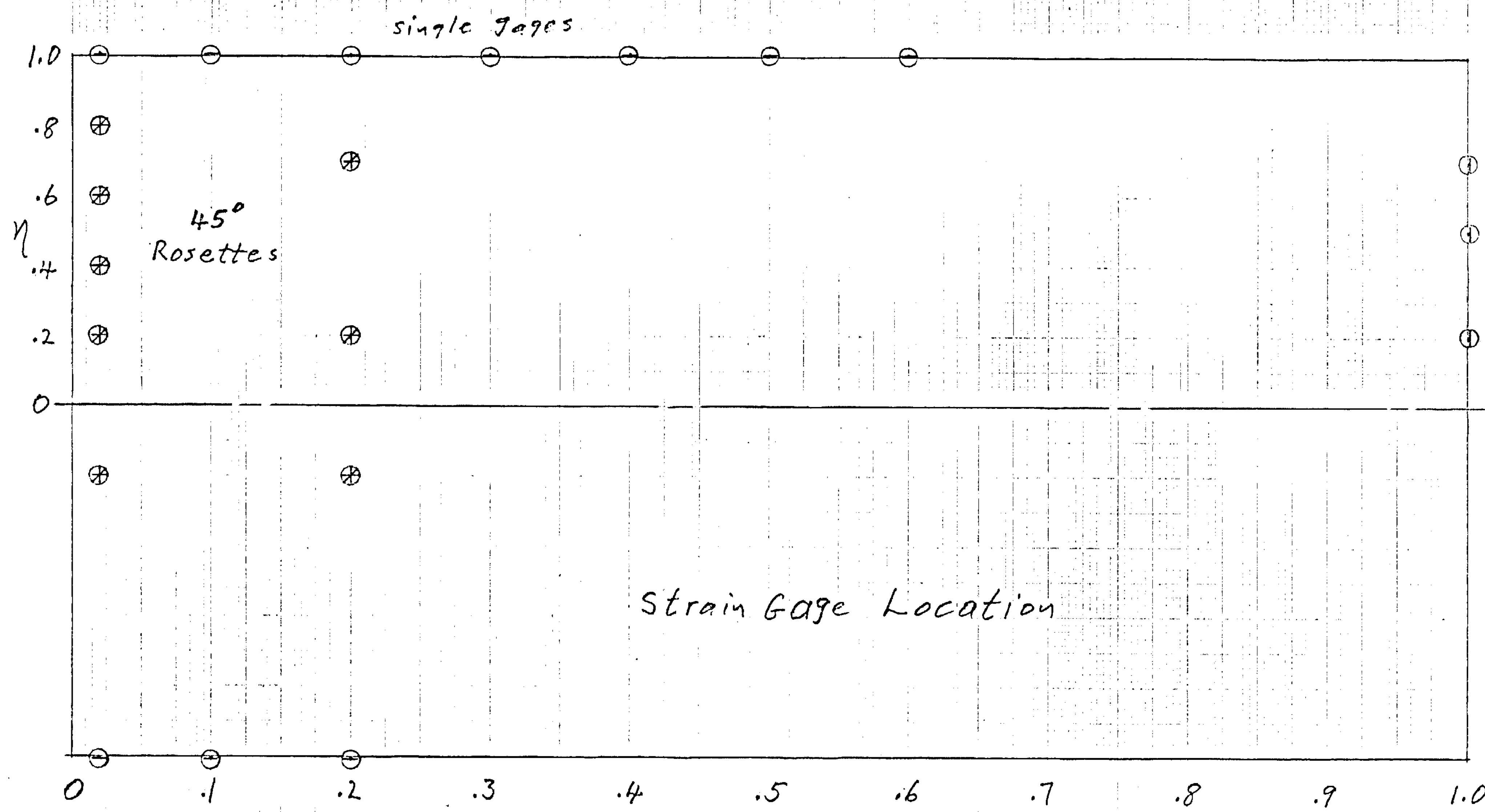
single gages
45° Rosettes
η
1.0
.8
.6
.4
.2
0
.1
.2
.3
.4
.5
.6
.7
.8
.9
1.0
Strain Gage Location

Fig. 4

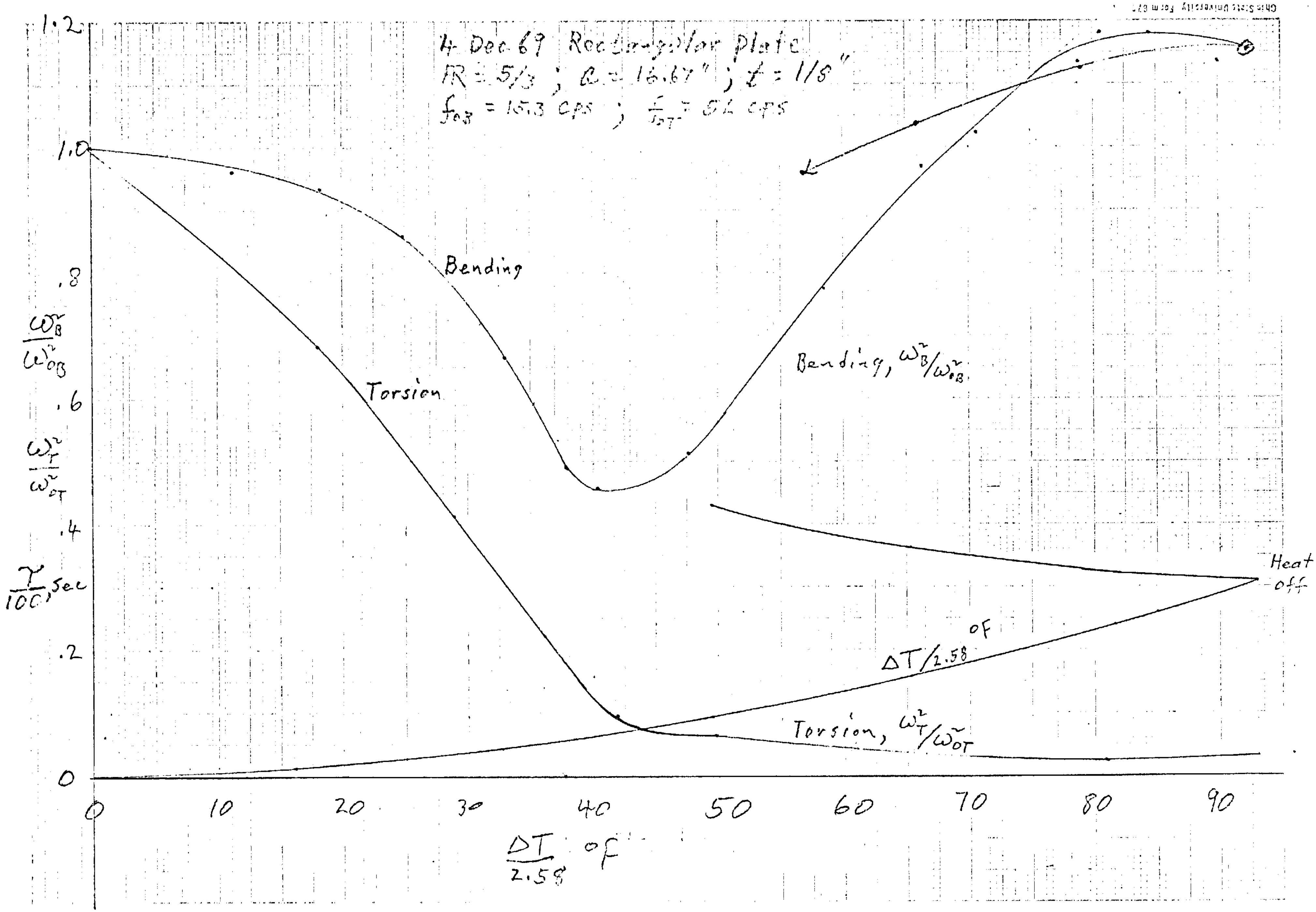

4 Dec 69 Rectangular plate
R = 5/3 ; a = 16.67" ; t = 1/8"
Bending
Torsion
Bending, ω_B^2/ω_{0B}^2
Torsion, ω_T^2/ω_{0T}^2
$\Delta T/2.58$ °F
Heat off
$\frac{\omega_B^2}{\omega_{0B}^2}$
$\frac{\omega_T^2}{\omega_{0T}^2}$
$\frac{\tau}{100}$, sec
$\frac{\Delta T}{2.58}$ °F

Fig. 5

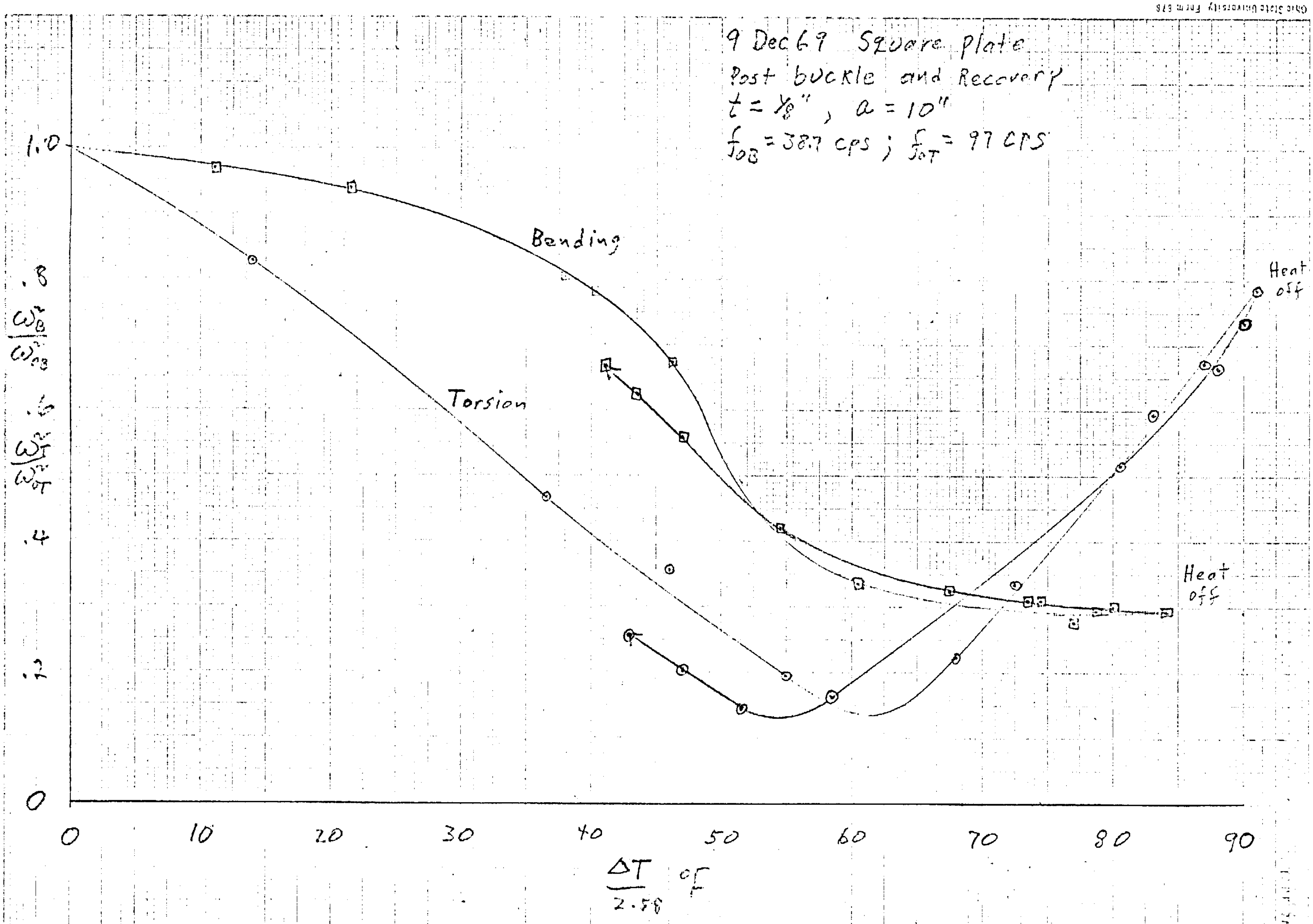

9 Dec 69 Square plate
Post buckle and Recovery
$t = 1/8''$, $a = 10''$
$f_{0B} = 38.7$ cps ; $f_{0T} = 97$ CPS
Bending
Torsion
Heat off
Heat off
1.0
.8
.6
.4
.2
0
$\frac{\omega_B^2}{\omega_{0B}^2}$
$\frac{\omega_T^2}{\omega_{0T}^2}$
0
10
20
30
40
50
60
70
80
90
$\frac{\Delta T}{2.58}$ °F

Fig. 6

Analytical
Effect of Frequency Ratio
on
Post-buckling Behavior

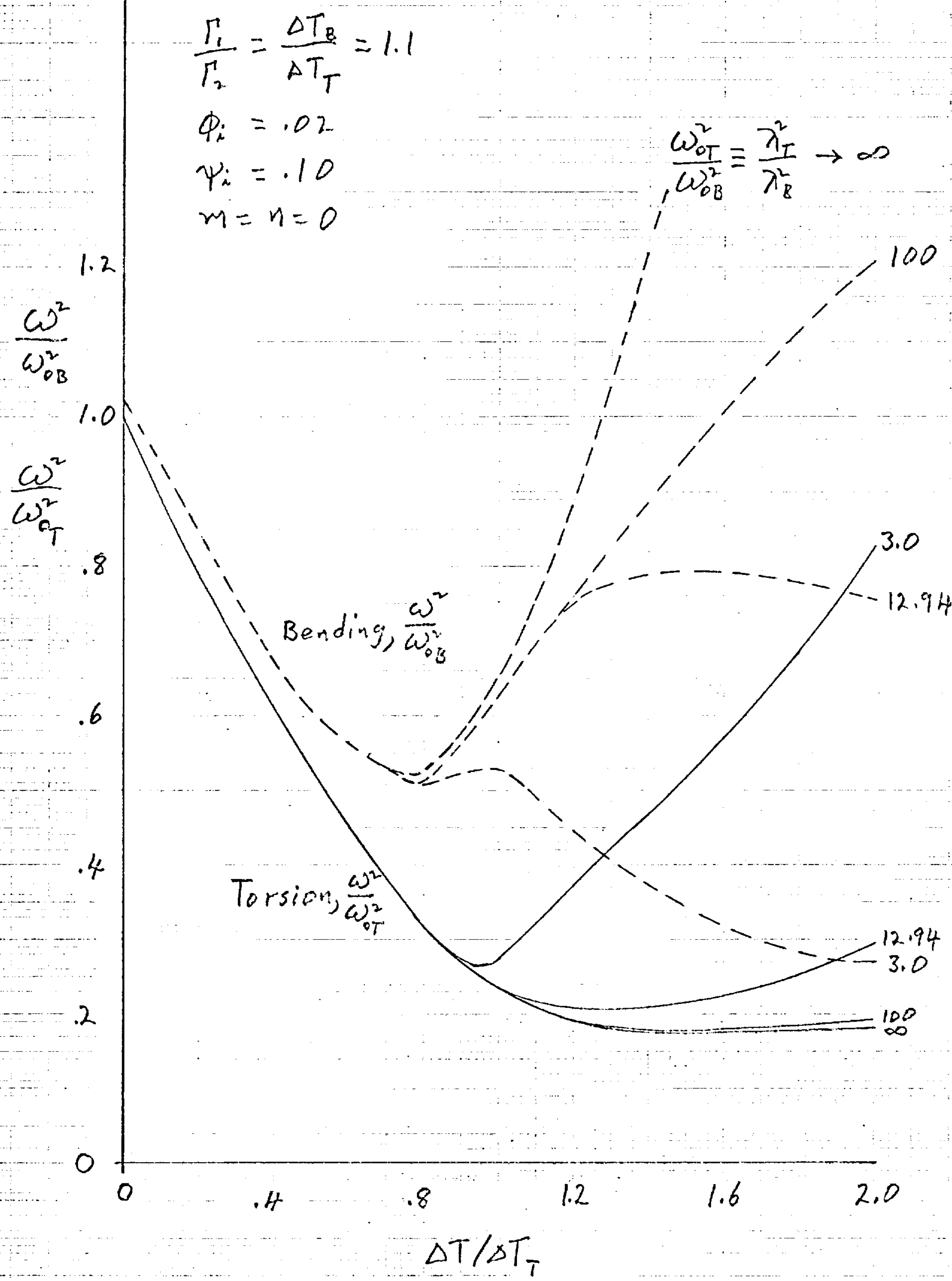

Fig. 7

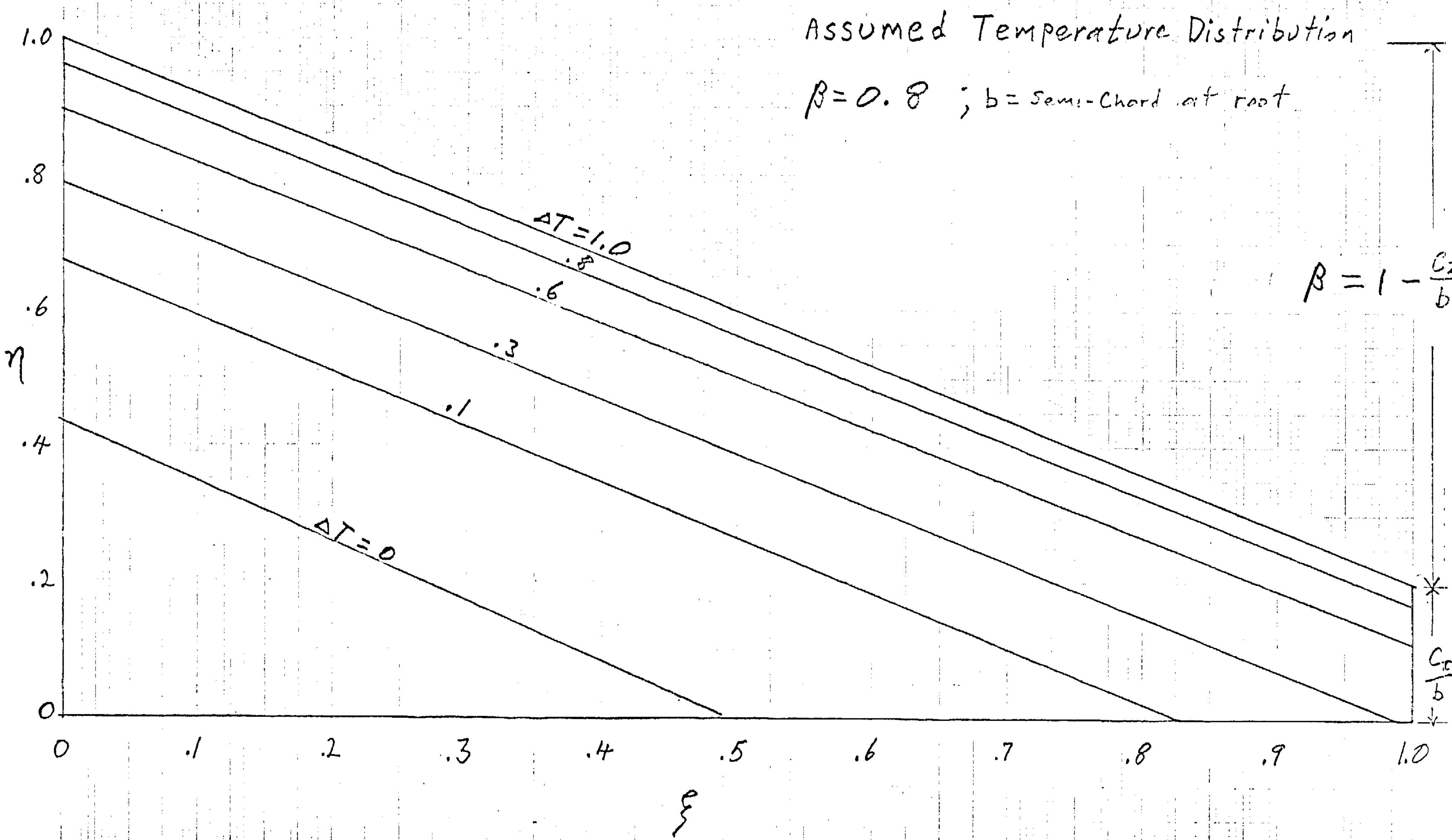
Assumed Temperature Distribution
$\beta = 0.8$; b = Semi-Chord at root
$\beta = 1 - \frac{C_2}{b}$
$\Delta T = 1.0$
.8
.6
.3
.1
$\Delta T = 0$
η
ξ
1.0
.8
.6
.4
.2
0
.1
.2
.3
.4
.5
.6
.7
.8
.9
1.0

Fig. 8

RELATION BETWEEN THE VARIOUS FACETS OF THE PROBLEM

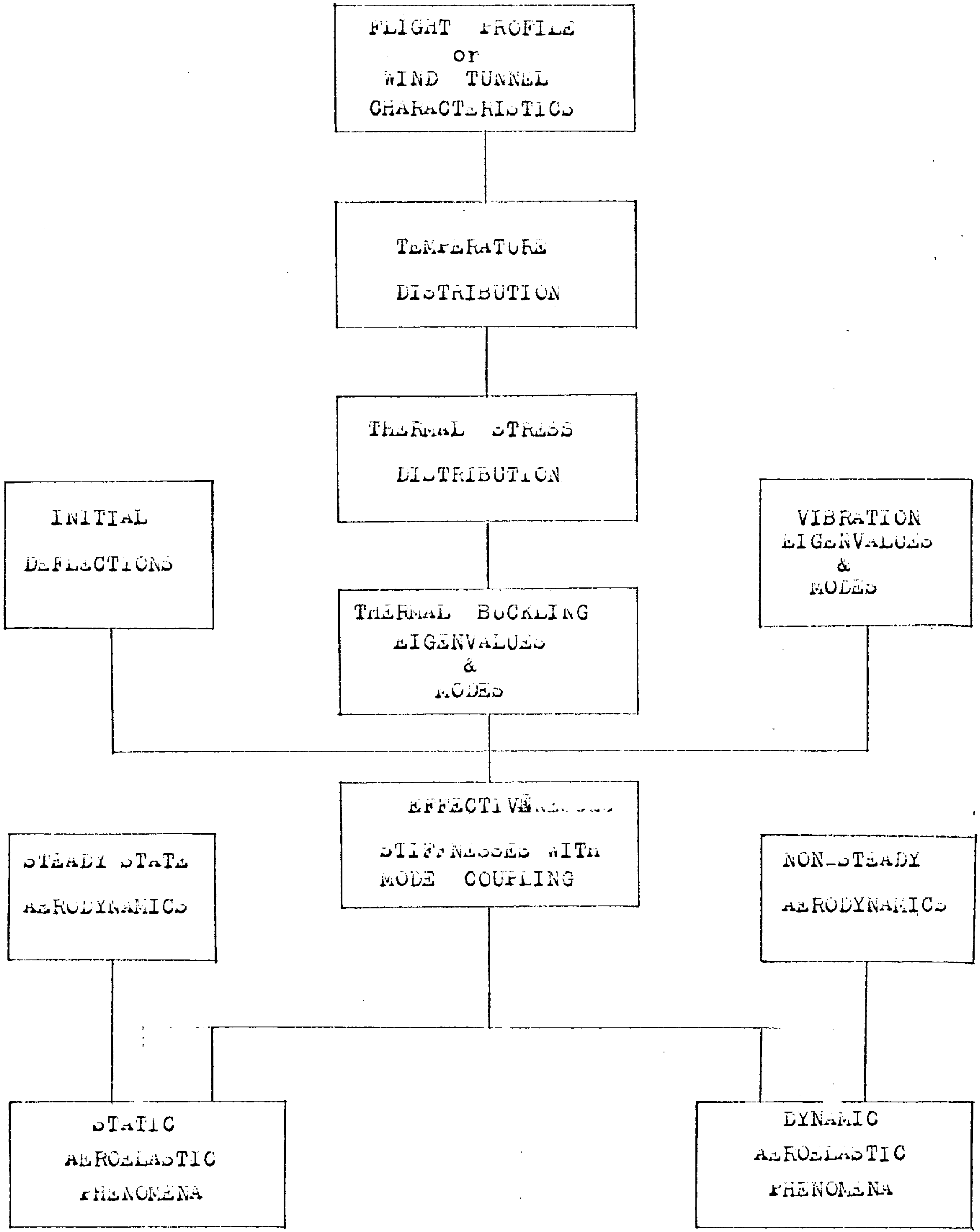

FIG. 9

AR \ β		-1.0	-.5	0	0.4	0.8	1.0
.5	λ_B^2	7.402	9.386	12.269	15.167	20.888	31.249
	λ_T^2	11.420	16.479	28.050	46.397	90.027	131.17
	λ_T^2/λ_B^2	1.543	1.756	2.286	3.059	4.310	4.198
.75	λ_B^2	7.965	9.576	12.2	15.602	23.319	36.156
	λ_T^2	21.826	29.085	46.56	78.335	154.419	215.37
	λ_T^2/λ_B^2	2.740	3.031	3.816	5.021	6.625	5.957
1.0	λ_B^2	8.042	9.595	12.137	15.792	24.701	39.486
	λ_T^2	33.669	45.621	70.123	116.82	229.20	315.09
	λ_T^2/λ_B^2	4.186	4.754	5.178	7.397	9.279	7.98
1.667	λ_B^2	7.978		12.003	15.922	26.242	43.935
	λ_T^2	80.387		155.859	250.51	477.044	636.81
	λ_T^2/λ_B^2	10.5		12.985	13.703	18.179	14.51
2.0	λ_B^2	7.887	9.460	11.953	15.927	26.557	44.569
	λ_T^2	123.49	149.86	212.62	335.58	628.22	828.34
	λ_T^2/λ_B^2	15.657	15.841	17.788	21.07	23.656	18.586
4.0	λ_B^2	7.873	9.165	11.812	15.877	27.13	47.115
	λ_T^2	408.92	557.28	758.49	1124.6	1915.9	2378.5
	λ_T^2/λ_B^2	51.805	60.804	64.214	70.832	70.619	50.493

TABLE I

Vibration Eigenvalues and Ratios

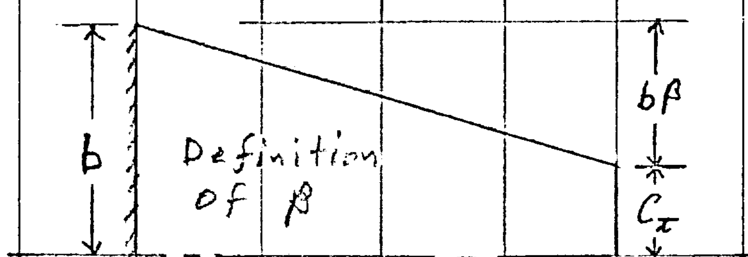

$$\beta = 1 - \frac{C_I}{b}$$

AR	β	-1.0	-.5	0	.4	.8	1.0
.5	K_B	492.62	266.98	103.07	43.53	19.987	17.19
	K_T	191.53	221.9	95.49	41.228	18.55	14.41
	Γ_B/Γ_T	2.573	1.203	1.079	1.056	1.078	1.193
.75	K_B	855.64	535.88	261.28	131.77	63.88	45.99
	K_T	521.82	453.64	239.4	122.1	59.17	41.05
	Γ_B/Γ_T	1.64	1.18	1.091	1.079	1.079	1.12
1.0	K_B	1521.8	1041.2	563.21	307.6	158.88	105.18
	K_T	1154.0	914.2	515.64	285.08	142.32	96.68
	Γ_B/Γ_T	1.32	1.139	1.092	1.079	1.116	1.088
1.667	K_B			2673.6	1597.9	845.1	558.04
	K_T			2596.7	1543.1	774.4	501.4
	Γ_B/Γ_T			1.0296	1.0355	1.091	1.113
2.0	K_B	8305.6	7918	4946	3024	1570	1110.5
	K_T	11,280	5949	4953	2971	1473	928.7
	Γ_B/Γ_T	.73626	1.331	.9986	1.018	1.0655	1.196
4.0	K_B	134,852	94,557	54,188	39,080	19,694	11,431
	K_T	145,144	106,143	69,138	40,276	18,326	10,768
	Γ_B/Γ_T	.9291	.891	.7838	.9703	1.0747	1.0616

TABLE II

Thermal Buckling Eigenvalues and Ratios

APPENDIX I

The total energy of a plate may be expressed as the energy of the perfect plate plus the change in energy due to arbitrary initial deflections as follows:*

$$\delta\Pi = \delta\Bigg\{\iint \frac{D}{2}\left[\left(\frac{\partial^2 w}{\partial x^2}\right)^2 + \left(\frac{\partial^2 w}{\partial y^2}\right)^2 + 2\nu\,\frac{\partial^2 w}{\partial x^2}\frac{\partial^2 w}{\partial y^2} + 2(1-\nu)\left(\frac{\partial^2 w}{\partial x\,\partial y}\right)^2\right]dx\,dy$$

$$+\frac{1}{2}\iint\left[\frac{\partial^2 F}{\partial y^2}\left(\frac{\partial w}{\partial x}\right)^2 + \frac{\partial^2 F}{\partial x^2}\left(\frac{\partial w}{\partial y}\right)^2 - 2\,\frac{\partial^2 F}{\partial x\,\partial y}\frac{\partial w}{\partial x}\frac{\partial w}{\partial y}\right]dx\,dy$$

$$-\frac{1}{2}\iint\frac{1}{Eh}\left[\left(\frac{\partial^2 F}{\partial y^2}\right)^2 + \left(\frac{\partial^2 F}{\partial x^2}\right)^2 - 2\nu\,\frac{\partial^2 F}{\partial x^2}\frac{\partial^2 F}{\partial y^2} + 2(1+\nu)\left(\frac{\partial^2 F}{\partial x\,\partial y}\right)^2\right]dx\,dy$$

$$-\iint \alpha T\left[\frac{\partial^2 F}{\partial x^2} + \frac{\partial^2 F}{\partial y^2}\right]dx\,dy - \iint Z\,w\,dx\,dy + \int_C \left(P_x u + P_y v\right)d\ell$$

$$+\iint \frac{D}{2}\left[\left(\frac{\partial^2 w_i}{\partial x^2}\right)^2 + \left(\frac{\partial^2 w_i}{\partial y^2}\right)^2 + 2\nu\,\frac{\partial^2 w_i}{\partial x^2}\frac{\partial^2 w_i}{\partial y^2} + 2(1-\nu)\left(\frac{\partial^2 w_i}{\partial x\,\partial y}\right)^2\right]dx\,dy$$

$$-\iint D\left[\frac{\partial^2 w}{\partial x^2}\frac{\partial^2 w_i}{\partial x^2} + \frac{\partial^2 w}{\partial y^2}\frac{\partial^2 w_i}{\partial y^2} + \nu\left(\frac{\partial^2 w}{\partial x^2}\frac{\partial^2 w_i}{\partial y^2} + \frac{\partial^2 w}{\partial y^2}\frac{\partial^2 w_i}{\partial x^2}\right) + 2(1-\nu)\frac{\partial^2 w}{\partial x\,\partial y}\frac{\partial^2 w_i}{\partial x\,\partial y}\right]dx\,dy$$

$$-\iint\frac{1}{2}\left[\frac{\partial^2 F}{\partial y^2}\left(\frac{\partial w_i}{\partial x}\right)^2 + \frac{\partial^2 F}{\partial x^2}\left(\frac{\partial w_i}{\partial y}\right)^2 - 2\,\frac{\partial^2 F}{\partial x\,\partial y}\frac{\partial w_i}{\partial x}\frac{\partial w_i}{\partial y}\right]dx\,dy$$

$$+\iint Z\,w_i\,dx\,dy\Bigg\} = 0.$$

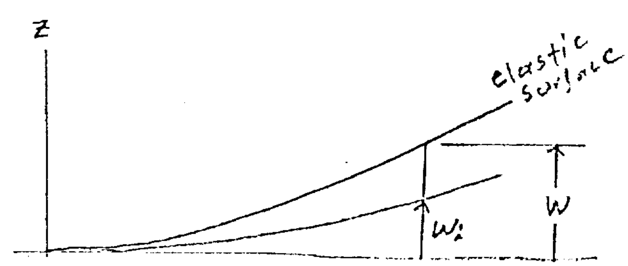

$$W_{elastic} = W - W_i$$

* See page 7 of the attached paper, "Modal Coupling in Thermally Stressed Plates".

Assuming W to be a linear combination of the small deflection modes as in the attached paper and following the definition of terms and procedures of that paper gives frequency equations and static deflection equations of the same form as in that paper:

$$\left(\frac{\omega^2}{\omega_{o2}^2}\right)_{1,2} = \frac{1}{2}\left\{C_2 + \frac{\omega_{o1}^2}{\omega_{o2}^2}C_1 \mp \left[\left(C_2 - \frac{\omega_{o1}^2}{\omega_{o2}^2}C_1\right)^2 + 16\frac{\omega_{o1}^2}{\omega_{o2}^2}\Psi^2\Phi^2\right]^{\frac{1}{2}}\right\}$$

$$\Psi^3 + \Psi\left[C_1 - 3\Phi^2\right] = \psi_o + \psi_i$$

$$\Phi^3 + \Phi\left[C_2 - 3\Phi^2\right] = \phi_o + \phi_i$$

Except that now,

$$C_1 = 1 - \frac{\Gamma}{\Gamma_1} + 3\Psi^2 + \frac{\Gamma_2}{\Gamma_1}\Phi^2 - \frac{I_{13}}{\Gamma_1} - \frac{I_{10}}{\Gamma_1}$$

$$C_2 = 1 - \frac{\Gamma}{\Gamma_2} + 3\Phi^2 + \frac{\Gamma_1}{\Gamma_2}\Psi^2 - \frac{I_{13}}{\Gamma_2} - \frac{I_{10}}{\Gamma_2}$$

where,

$$I_{13} = \iint\left[\frac{\partial^2 F}{\partial x^2}\left(\frac{\partial w_i}{\partial y}\right)^2 + \frac{\partial^2 F}{\partial y^2}\left(\frac{\partial w_i}{\partial x}\right)^2 - 2\frac{\partial^2 F}{\partial x \partial y}\frac{\partial w_i}{\partial x}\frac{\partial w_i}{\partial y}\right]dx\,dy$$

$$\psi_i = \frac{I_{11}}{I_2}\left(\frac{I_3}{2\Gamma_1}\right)^{\frac{1}{2}}$$

$$\phi_i = \frac{I_{12}}{I_6}\left(\frac{I_7}{2\Gamma_2}\right)^{\frac{1}{2}}$$

$$I_{11} = \iint D \left\{ \frac{\partial^2 w_1}{\partial x^2}\frac{\partial^2 w_i}{\partial x^2} + \frac{\partial^2 w_1}{\partial y^2}\frac{\partial^2 w_i}{\partial y^2} + \nu\left(\frac{\partial^2 w_1}{\partial x^2}\frac{\partial^2 w_i}{\partial y^2} + \frac{\partial^2 w_1}{\partial y^2}\frac{\partial^2 w_i}{\partial x^2}\right) + 2(1-\nu)\frac{\partial^2 w_1}{\partial x \partial y}\frac{\partial^2 w_i}{\partial x \partial y} \right\} dx\, dy$$

$$I_{12} = \iint D \left\{ \frac{\partial^2 w_2}{\partial x^2}\frac{\partial^2 w_i}{\partial x^2} + \frac{\partial^2 w_2}{\partial y^2}\frac{\partial^2 w_i}{\partial y^2} + \nu\left(\frac{\partial^2 w_2}{\partial x^2}\frac{\partial^2 w_i}{\partial y^2} + \frac{\partial^2 w_2}{\partial y^2}\frac{\partial^2 w_i}{\partial x^2}\right) + 2(1-\nu)\frac{\partial^2 w_2}{\partial x \partial y}\frac{\partial^2 w_i}{\partial x \partial y} \right\} dx\, dy$$

A comparison of these equations with those of the attached report shows that:

$$I_{13} = \Gamma_1 \psi_i + \Gamma_2 \phi_i \, .$$

I_2, I_3, I_6, and I_7 are as defined in the attached paper.

The application of the theory to arbitrary imperfections may be evaluated by the following steps:

1. Measure the initial shape of a plate.
2. Obtain the frequency at some measured temperature distribution and magnitude.
3. Obtain the buckling eigenvalues for the perfect plate, Γ_1 and Γ_2, using the temperature distribution at which the frequency was measured. At this time, all integrals involved in the linear solution may be evaluated.
4. Evaluate I_{11} and I_{12} from the measured shape data and perfect plate modes.
5. Evaluate ψ_i and ϕ_i from their definitions.
6. Evaluate I_{13} from $I_{13} = \Gamma_1 \psi_i + \Gamma_2 \phi_i$.
7. Use I_{11}, I_{12}, and I_{13} in the non-linear equations to

calculate the frequency response for the temperature magnitude at which the frequency was measured.

8. Compare analytical with experimental results.

Appendix II

Development of Equations for a Parametric Flutter Analysis

The basic equations to be considered are Equations (6) and (7) from Attachment 1 which are repeated here

$$\left.\begin{aligned}
&\frac{\ddot{\psi}}{\omega_{01}^2} + \psi^3 + \psi\left[1 - \frac{T}{T_1} - \psi_i^2 + \frac{T_2}{T_1}(\phi^2 - \phi_i^2) - \frac{I_{10}}{\omega_{01}^2 I_9}\right] = \psi_0 + \psi_i \\
&\frac{\ddot{\phi}}{\omega_{02}^2} + \phi^3 + \phi\left[1 - \frac{T}{T_2} - \phi_i^2 + \frac{T_1}{T_2}(\psi^2 - \psi_i^2) - \frac{I_{10}}{\omega_{02}^2 I_9}\right] = \phi_0 + \phi_i
\end{aligned}\right\} \quad (1)$$

with

$$\left.\begin{aligned}
\psi_0 &= \frac{1}{T_1}\sqrt{\frac{I_9}{I_2}}\int_A \Delta p(\psi,\phi)\, W_1\, dA + \bar{\psi}_0 \\
\phi_0 &= \frac{1}{T_2}\sqrt{\frac{I_9}{I_6}}\int_A \Delta p(\psi,\phi)\, W_2\, dA + \bar{\phi}_0
\end{aligned}\right\} \quad (2)$$

and

$$\left.\begin{aligned}
\bar{\psi}_0 &= \frac{1}{T_1}\sqrt{\frac{I_9}{I_2}}\int_A \Delta p(\psi_0,\phi_0)\, W_1\, dA \\
\bar{\phi}_0 &= \frac{1}{T_2}\sqrt{\frac{I_9}{I_6}}\int_A \Delta p(\psi_0,\phi_0)\, W_2\, dA
\end{aligned}\right\} \quad (3)$$

The pressure in Equations (2) and (3) is obtained from modified Piston Theory as*

$$\Delta p(\psi,\phi) = -\frac{4\delta}{\sqrt{M^2 - \chi^2}}\left[\sqrt{\frac{T_1}{I_3}}\left\{\psi W_{1_x} + \frac{W_1}{V}\dot{\psi}\right\} + \sqrt{\frac{T_2}{I_7}}\left\{\phi W_{2_x} + \frac{W_2}{V}\dot{\phi}\right\}\right] \quad (4)$$

---

* Only the first term of the nonlinear pressure expression is used here.

with

$$\lambda^2 = \frac{\sec^2 \Lambda}{(1+k)^4} \tag{5}$$

where in Equations (4) and (5)

M - Mach Number (V/a)

k - Reduced Frequency $\left(\frac{\omega_{01} b}{V}\right)$

b - Semi-root Chord

V - Free Stream Velocity

Λ - Leading Edge Sweepback Angle

q - Dynamic Pressure $(\rho V^2/2)$

ρ - Fluid Density

with the remaining terms defined in Attachment 1.

The integrals resulting from the evaluation of Equations (2) and (3) may be written

$$\left.\begin{aligned} J_{r,s} &= \frac{1}{b}\int_A W_r W_{s_x}\, dA \\ K_{r,s} &= \frac{1}{b^2}\int_A W_r W_s\, dA \end{aligned} \qquad r,s = 1,2 \right\} \tag{6}$$

Equations (2) may now be expressed as

$$\left.\begin{aligned} \psi_0 &= \bar{\psi}_0 - \frac{b}{T_1}\sqrt{\frac{I_9}{I_2}}\,\frac{4q}{\sqrt{M^2-\lambda^2}}\left\{\sqrt{\frac{T_1}{I_3}}\left[\psi J_{1,1} + \frac{b}{V}K_{1,1}\dot{\psi}\right] + \sqrt{\frac{T_2}{I_7}}\left[\phi J_{1,2} + \frac{b}{V}K_{1,2}\dot{\phi}\right]\right\} \\ \phi_0 &= \bar{\phi}_0 - \frac{b}{T_2}\sqrt{\frac{I_9}{I_6}}\,\frac{4q}{\sqrt{M^2-\lambda^2}}\left\{\sqrt{\frac{T_1}{I_3}}\left[\psi J_{2,1} + \frac{b}{V}K_{1,2}\dot{\psi}\right] + \sqrt{\frac{T_2}{I_7}}\left[\phi J_{2,2} + \frac{b}{V}K_{2,2}\dot{\phi}\right]\right\} \end{aligned}\right\} \tag{7}$$

It is convenient to rewrite Equations (7) as

$$\left.\begin{aligned} \psi_0 &= \bar{\psi}_0 - [\, a_{1,1}\psi + a_{1,2}\phi + b_{1,1}\dot{\psi} + b_{1,2}\dot{\phi}\,] \\ \phi_0 &= \bar{\phi}_0 - [\, a_{2,1}\psi + a_{2,2}\phi + b_{2,1}\dot{\psi} + b_{2,2}\dot{\phi}\,] \end{aligned}\right\} \quad (8)$$

where

$$\left.\begin{aligned} a_{1,1} &= \frac{4\delta b}{T_1\sqrt{M^2-\lambda^2}}\sqrt{\frac{I_9 T_1}{I_2 I_3}}\; J_{1,1} \\ a_{1,2} &= \frac{4\delta b}{T_1\sqrt{M^2-\lambda^2}}\sqrt{\frac{I_9 T_1}{I_2 I_3}}\sqrt{\frac{T_2}{T_1}}\sqrt{\frac{I_3}{I_7}}\; J_{1,2} \\ a_{2,1} &= \frac{4\delta b}{T_1\sqrt{M^2-\lambda^2}}\left(\frac{T_1}{T_2}\right)\sqrt{\frac{I_9 T_1}{I_2 I_3}}\sqrt{\frac{I_2}{I_6}}\; J_{2,1} \\ a_{2,2} &= \frac{4\delta b}{T_1\sqrt{M^2-\lambda^2}}\left(\frac{T_1}{T_2}\right)\sqrt{\frac{I_9 T_1}{I_2 I_3}}\sqrt{\frac{T_2}{T_1}}\sqrt{\frac{I_2}{I_6}}\; J_{2,2} \end{aligned}\right\} \quad (9)$$

and

$$\left.\begin{aligned} b_{1,1} &= \frac{4b\delta}{T_1\sqrt{M^2-\lambda^2}}\left(\frac{b}{V}\right)\sqrt{\frac{I_9 T_1}{I_2 I_3}}\; K_{1,1} \\ b_{1,2} &= \frac{4b\delta}{T_1\sqrt{M^2-\lambda^2}}\left(\frac{b}{V}\right)\sqrt{\frac{I_9 T_1}{I_2 I_3}}\sqrt{\frac{T_2}{T_1}}\sqrt{\frac{I_3}{I_7}}\; K_{1,2} \\ b_{2,1} &= \frac{4b\delta}{T_1\sqrt{M^2-\lambda^2}}\left(\frac{b}{V}\right)\left(\frac{T_1}{T_2}\right)\sqrt{\frac{I_9 T_1}{I_2 I_3}}\sqrt{\frac{I_2}{I_6}}\; K_{1,2} \\ b_{2,2} &= \frac{4b\delta}{T_1\sqrt{M^2-\lambda^2}}\left(\frac{b}{V}\right)\left(\frac{T_1}{T_2}\right)\sqrt{\frac{I_9 T_1}{I_2 I_3}}\sqrt{\frac{T_2}{T_1}}\sqrt{\frac{I_2}{I_6}}\; K_{2,2} \end{aligned}\right\} \quad (10)$$

Consider now, as in Attachment 1

$$\left.\begin{aligned} \psi &= \epsilon_\psi + \bar{\psi} \quad ; \quad \dot{\psi} = \dot{\epsilon}_\psi \\ \phi &= \epsilon_\phi + \bar{\phi} \quad ; \quad \dot{\phi} = \dot{\epsilon}_\phi \end{aligned}\right\} \quad (11)$$

and obtain the following steady-state equilibrium equations which result when $\epsilon_\psi = \epsilon_\phi = 0$.

$$\bar{\varphi}^3 + \bar{\varphi}\left[1 - \frac{\Pi}{\Pi_1} - \varphi_i^2 + \frac{\Pi_2}{\Pi_1}(\bar{\phi}^2 - \phi_i^2) + a_{1,1} - \frac{I_{10}}{\omega_{01}^2 I_q}\right] + a_{1,2}\,\bar{\phi} = \varphi_0 + \varphi_i$$
$$\bar{\phi}^3 + \bar{\phi}\left[1 - \frac{\Pi}{\Pi_2} - \phi_i^2 + \frac{\Pi}{\Pi_2}(\bar{\varphi}^2 - \varphi_i^2) + a_{2,2} - \frac{I_{10}}{\omega_{02}^2 I_q}\right] + a_{2,1}\,\bar{\varphi} = \bar{\phi}_0 + \phi_i \qquad (12)$$

Substract the above steady-state equations from the general equations and linearize the resulting equations in ϵ_ϕ and ϵ_φ to get

$$\frac{\ddot{\epsilon}_\varphi}{\omega_{01}^2} + \epsilon_\varphi\left[1 - \frac{\Pi}{\Pi_1} - \varphi_i^2 + \frac{\Pi_2}{\Pi_1}(\bar{\phi}^2 - \phi_i^2) + a_{1,1} - \frac{I_{10}}{\omega_{01}^2 I_q} + 3\bar{\varphi}^2\right]$$
$$+ \epsilon_\phi\left[2\frac{\Pi_2}{\Pi_1}\bar{\varphi}\bar{\phi} + a_{1,2}\right] + b_{1,1}\dot{\epsilon}_\varphi + b_{1,2}\dot{\epsilon}_\phi = 0$$
$$\frac{\ddot{\epsilon}_\phi}{\omega_{02}^2} + \epsilon_\phi\left[1 - \frac{\Pi}{\Pi_2} - \phi_i^2 + \frac{\Pi_1}{\Pi_2}(\bar{\varphi}^2 - \varphi_i^2) + a_{2,2} - \frac{I_{10}}{\omega_{02}^2 I_q} + 3\bar{\phi}^2\right]$$
$$+ \epsilon_\varphi\left[2\frac{\Pi_1}{\Pi_2}\bar{\varphi}\bar{\phi} + a_{2,1}\right] + b_{2,1}\dot{\epsilon}_\varphi + b_{2,2}\dot{\epsilon}_\phi = 0 \qquad (13)$$

Again for convenience of notation, rewrite Equations (12) and (13) as

$$F(\bar{\phi},\bar{\varphi}) = \bar{\varphi}^3 + (A1)\bar{\varphi} + (A2)\bar{\phi} - (A4) = 0$$
$$G(\bar{\phi},\bar{\varphi}) = \bar{\phi}^3 + (B1)\bar{\phi} + (B2)\bar{\varphi} - (B4) = 0 \qquad (14)$$

and

$$\frac{\ddot{\epsilon}_\varphi}{\omega_{01}^2} + (A5)\dot{\epsilon}_\varphi + (A6)\dot{\epsilon}_\phi + (A7)\epsilon_\varphi + (A8)\epsilon_\phi = 0$$
$$\frac{\ddot{\epsilon}_\phi}{\omega_{01}^2} + (B5)\dot{\epsilon}_\phi + (B6)\dot{\epsilon}_\varphi + (B7)\epsilon_\phi + (B8)\epsilon_\varphi = 0 \qquad (15)$$

where in Equations (14)

$$
\left.
\begin{aligned}
(A1) &= \left[1 - \frac{T}{T_1} - \psi_i^2 + \frac{T_2}{T_1}(\bar{\phi}^2 - \phi_i^2) + \frac{4\delta b}{T_1\sqrt{M^2-\lambda^2}}\sqrt{\frac{I_9 T_1}{I_2 I_3}}\, J_{1,1} - \frac{I_{10}}{\omega_{01}^2 I_9}\right] \\
(B1) &= \left[1 - \frac{T}{T_2} - \phi_i^2 + \frac{T_1}{T_2}(\bar{\psi}^2 - \psi_i^2) + \frac{4\delta b}{T_1\sqrt{M^2-\lambda^2}}\sqrt{\frac{I_9 T_1}{I_2 I_3}}\sqrt{\frac{T_1}{T_2}}\sqrt{\frac{I_2}{I_6}}\, J_{2,2} - \frac{I_{10}}{\omega_{02}^2 I_9}\right] \\
(A2) &= \frac{4\delta b}{T_1\sqrt{M^2-\lambda^2}}\sqrt{\frac{I_9 T_1}{I_2 I_3}}\sqrt{\frac{T_1}{T_2}}\sqrt{\frac{I_3}{I_7}}\, J_{1,2} \\
(B2) &= \frac{4\delta b}{T_1\sqrt{M^2-\lambda^2}}\sqrt{\frac{I_9 T_1}{I_2 I_3}}\left(\frac{T_1}{T_2}\right)\sqrt{\frac{I_2}{I_6}}\, J_{2,1} \\
(A4) &= \bar{\psi}_0 + \psi_i \quad ; \quad (B4) = \bar{\phi}_0 + \phi_i
\end{aligned}
\right\} \quad (16)
$$

and in Equations (15)

$$
\left.
\begin{aligned}
(A5) &= \frac{4\delta b}{T_1\sqrt{M^2-\lambda^2}}\left(\frac{b}{V}\right)\sqrt{\frac{I_9 T_1}{I_2 I_3}}\, K_{1,1} \\
(B5) &= \frac{4\delta b}{T_1\sqrt{M^2-\lambda^2}}\left(\frac{b}{V}\right)\sqrt{\frac{I_9 T_1}{I_2 I_3}}\sqrt{\frac{T_1}{T_2}}\sqrt{\frac{I_2}{I_6}}\, K_{2,2} \\
(A6) &= \frac{4\delta b}{T_1\sqrt{M^2-\lambda^2}}\left(\frac{b}{V}\right)\sqrt{\frac{I_9 T_1}{I_2 I_3}}\sqrt{\frac{T_2}{T_1}}\sqrt{\frac{I_3}{I_7}}\, K_{1,2} \\
(B6) &= \frac{4\delta b}{T_1\sqrt{M^2-\lambda^2}}\left(\frac{b}{V}\right)\sqrt{\frac{I_9 T_1}{I_2 I_3}}\left(\frac{T_1}{T_2}\right)\sqrt{\frac{I_2}{I_6}}\, K_{1,2} \\
(A7) &= (A1) + 3\bar{\psi}^2 \quad ; \quad (B7) = (B1) + 3\bar{\phi}^2 \\
(A8) &= 2\left(\frac{T_2}{T_1}\right)\bar{\psi}\bar{\phi} + (A2) \quad ; \quad (B8) = 2\left(\frac{T_1}{T_2}\right)\bar{\phi}\bar{\psi} + (B2)
\end{aligned}
\right\} \quad (17)
$$

Define now the following nondimensional parameters

$$
\left.
\begin{array}{llll}
P(1) = M & P(7) = \psi_i & P(13) = J_{2,1} & P(19) = \dfrac{I_{10}}{\omega_{01}^2 I_9} \\
P(2) = (\rho/\rho_0) & P(8) = \phi_i & P(14) = J_{2,2} & P(20) = \bar{\psi}_0 \\
P(3) = (T/T_1) & P(9) = \left(\dfrac{\omega_{01}}{\omega_{02}}\right) & P(15) = K_{1,1} & P(21) = \bar{\phi}_0 \\
P(4) = (T_2/T_1) & P(10) = \sqrt{\dfrac{I_1}{I_5}} & P(16) = K_{1,2} & \\
P(5) = (b\,\omega_{01}/a_0) & P(11) = J_{1,2} & P(17) = K_{2,2} & \\
P(6) = \left(\dfrac{2\rho_0 b^3}{I_1}\right) & P(12) = J_{1,1} & P(18) = \sec\Lambda &
\end{array}
\right\} \quad (18)
$$

In terms of the parameters of Equations (18), Equations (16) become

$$
\left.
\begin{aligned}
(A1) &= \left[1 - P(3) - P(7)^2 + P(4)\left\{\bar{\phi}^2 - P(8)^2\right\} - P(19) + \frac{P(2)\cdot P(6)\cdot P(12)}{D\cdot k^2}\right] \\
(B1) &= \left[1 - \frac{P(3)}{P(4)} - P(8)^2 + \left\{\frac{\bar{\psi}^2 - P(7)^2}{P(4)}\right\} - P(19)\cdot P(9)^2 + \frac{P(2)\cdot P(6)\cdot P(14)}{D\cdot k^2}\cdot\frac{P(9)P(10)}{\sqrt{P(4)}}\right] \\
(A2) &= P(2)\cdot P(4)\cdot P(6)\cdot P(9)\cdot P(10)\cdot P(11) \,/\, (D\cdot k^2) \\
(B2) &= P(2)\cdot P(4)\cdot P(6)\cdot P(9)\cdot P(10)\cdot P(13) \,/\, (D\cdot k^2) \\
(A4) &= P(20) + P(7) \quad ; \quad (B4) = P(21) + P(8)
\end{aligned}
\right\} \quad (19)
$$

and Equations (17) become

$$
\left.
\begin{aligned}
(A5) &= \frac{1}{\omega_{01}}\left[P(2)\cdot P(6)\cdot P(15) \,/\, D\cdot k\right] \\
(B5) &= \frac{1}{\omega_{01}}\left[P(2)\cdot P(6)\cdot P(9)\cdot P(10)\cdot P(17) \,/\, D\cdot k\cdot\sqrt{P(4)}\right] \\
(A6) &= \frac{1}{\omega_{01}}\left[P(2)\cdot P(4)\cdot P(6)\cdot P(9)\cdot P(10)\cdot P(16) \,/\, D\cdot k\right] \\
(B6) &= \frac{1}{\omega_{01}}\left[P(2)\cdot P(6)\cdot P(9)\cdot P(10)\cdot P(16) \,/\, D\cdot k\cdot\sqrt{P(4)}\right] \\
(A7) &= (A1) + 3\,\bar{\psi}^2 \quad ; \quad (B7) = (B1) + 3\,\bar{\phi}^2 \\
(A8) &= (A2) + 2\cdot\bar{\phi}\cdot\bar{\psi}\cdot P(4) \quad ; \quad (B8) = (B2) + \frac{2\cdot\bar{\phi}\cdot\bar{\psi}}{P(4)}
\end{aligned}
\right\} \quad (20)
$$

where in Equations (19) and (20)

$$
\left.
\begin{aligned}
k &= \frac{\omega_{01} b}{V} = \left(\frac{\omega_{01} b}{a_0}\right)\left(\frac{a_0}{a}\right)\left(\frac{a}{V}\right) = \frac{P(5)}{P(1)}\cdot P(2)^{\frac{\gamma-1}{2}} \\
D &= \left[P(1)^2 - \left\{\frac{P(18)}{(1+k)^2}\right\}^2\right]^{\frac{1}{2}}
\end{aligned}
\right\} \quad (21)
$$

Return now to Equations (15) and assume that $\bar{\psi}$ and $\bar{\phi}$ have been determined as solutions to Equations (14). The characteristic equation resulting from Equations (15) [having assumed solutions of the form e^{st}] is

$$\begin{vmatrix} \left[\left(\frac{s}{\omega_{01}}\right)^2 + \left(\frac{s}{\omega_{01}}\right)(\omega_{01} A5) + (A7)\right] & \left[\left(\frac{s}{\omega_{01}}\right)(\omega_{01} A6) + (A8)\right] \\ \left[\left(\frac{s}{\omega_{02}}\right)(\omega_{02} B6) + (B8)\right] & \left[\left(\frac{s}{\omega_{02}}\right)^2 + \left(\frac{s}{\omega_{02}}\right)(\omega_{02} B5) + (B7)\right] \end{vmatrix} = 0$$

or

$$\bar{s}^4 + C_4 \bar{s}^3 + C_3 \bar{s}^2 + C_2 \bar{s} + C_1 = 0 \tag{22}$$

where in Equation (22)

$$\left.\begin{aligned} \bar{s} &= \frac{s}{\omega_{01}} \\ C_4 &= (\omega_{01} A5) + \frac{(\omega_{01} B5)}{P(9)^2} \\ C_3 &= (A7) + \frac{1}{P(9)^2}\left\{(B7) + \left[(\omega_{01} A5)(\omega_{01} B5) - (\omega_{01} B6)(\omega_{01} A6)\right]\right\} \\ C_2 &= \frac{1}{P(9)^2}\left\{(B7)(\omega_{01} A5) + (A7)(\omega_{01} B5) - (A8)(\omega_{01} B6) - (B8)(\omega_{01} A6)\right\} \\ C_1 &= \frac{1}{P(9)^2}\left[(A7)(B7) - (A8)(B8)\right] \end{aligned}\right\} \tag{23}$$

Equations (14) and (22) were solved for the range of parameters indicated below

$$2.5 \leq M \leq 5$$

$$0.0 \leq \rho/\rho_0 \leq 1.0$$

$$0.0 \leq T/T_1 \leq 1.5$$

with the following assumed values for the remaining parameters

$T_2/T_1 = 0.8$	$\sqrt{\frac{I_1}{I_5}} = 1.5$	$K_{1,2} = 1.0$
$b\,\omega_{01}/a_0 = 0.2$	$J_{1,2} = 2.0$	$K_{2,2} = 0.7$
$\frac{2\rho_0 b^3}{I_1} = 0.572 \times 10^{-2}$	$J_{1,1} = 0.0$	$\sec\Lambda = 0.0$
$\Psi_i = 0.0$	$J_{2,1} = 0.0$	$\frac{I_{10}}{\omega_{01}^2 I_9} = 0.0$
$\Phi_i = 0.0$	$J_{2,2} = 1.0$	$\bar{\Psi}_0 = 0.0$
$\omega_{01}/\omega_{02} = 0.3$	$K_{1,1} = 2.0$	$\bar{\Phi}_0 = 0.0$

The reasonableness of the above list of parameters remains open for further study; the intention here is to indicate method and procedure assuming a valid parameter set is available.

Figure 1 of Appendix II basically defines the structure which is under investigation and is specifically the solutions to Equation (22) in the absence of any aerodynamics.

Figure 2 of Appendix II represents solutions to Equations (14) with density ratio as a parameter. These are the solutions which are used to evaluate the coefficients of Equation (22).

Figure 3 of Appendix II represents solutions to Equation (22) (The imaginary part of the solution only) with Mach Number as a parameter in the pre-buckled region. The real parts of the solution corresponding to these frequencies were all negative indicating dynamic stability.

Figure 4 of Appendix II contains the same type of information as did Figure 3 of Appendix II with the notable exception that in Figure 4 the post-buckled region is sampled. The real part of a solution became positive in the low density region as the frequencies approached each other, indicating a dynamic instability, and remained positive until a frequency attained its lower asymptotic value of 0.316. Beyond this point dynamic stability was again indicated.

Figure 5 of Appendix II shows the stability boundaries obtained in the manner previously indicated.

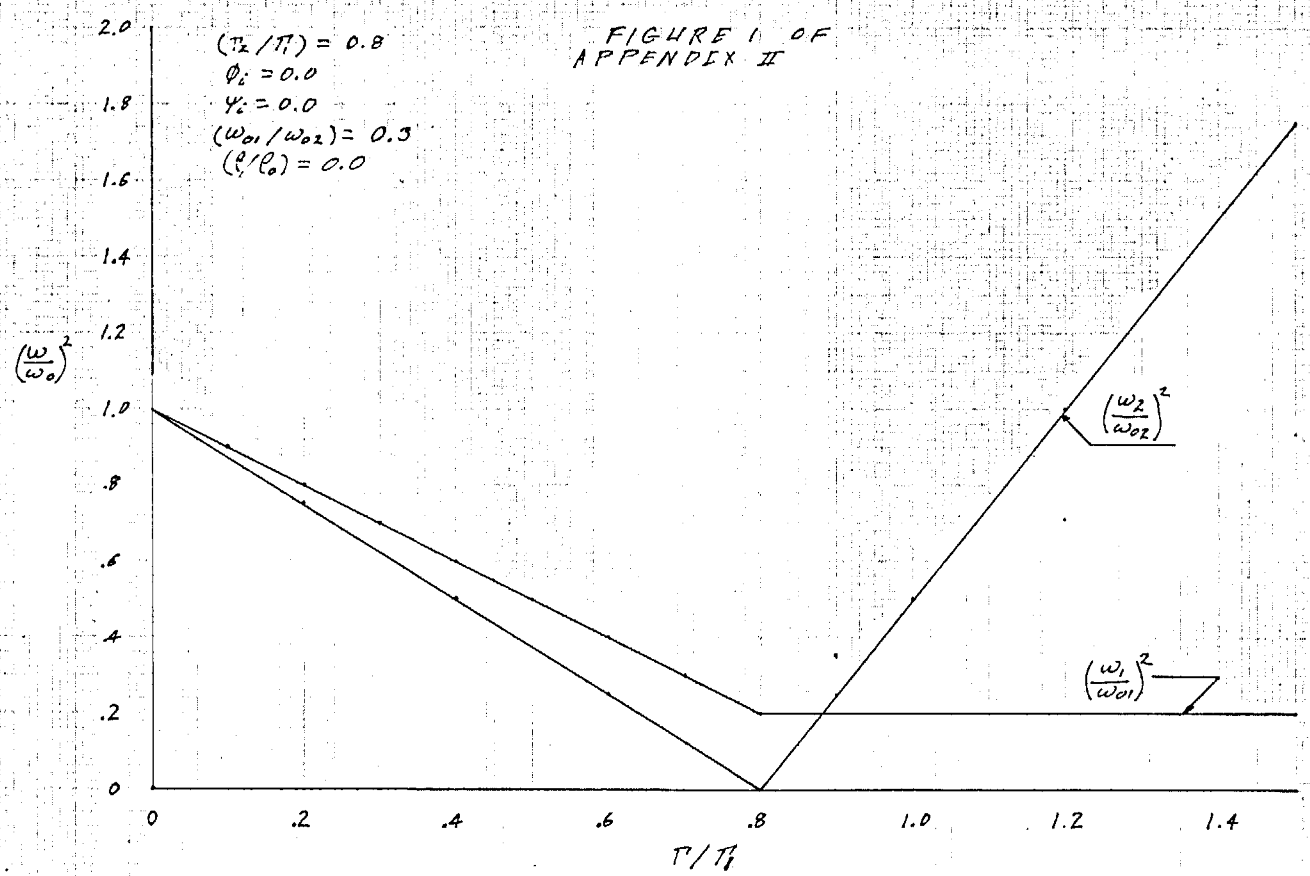

FIGURE 1 OF APPENDIX II

FORM 351-F-4 REV 10/67

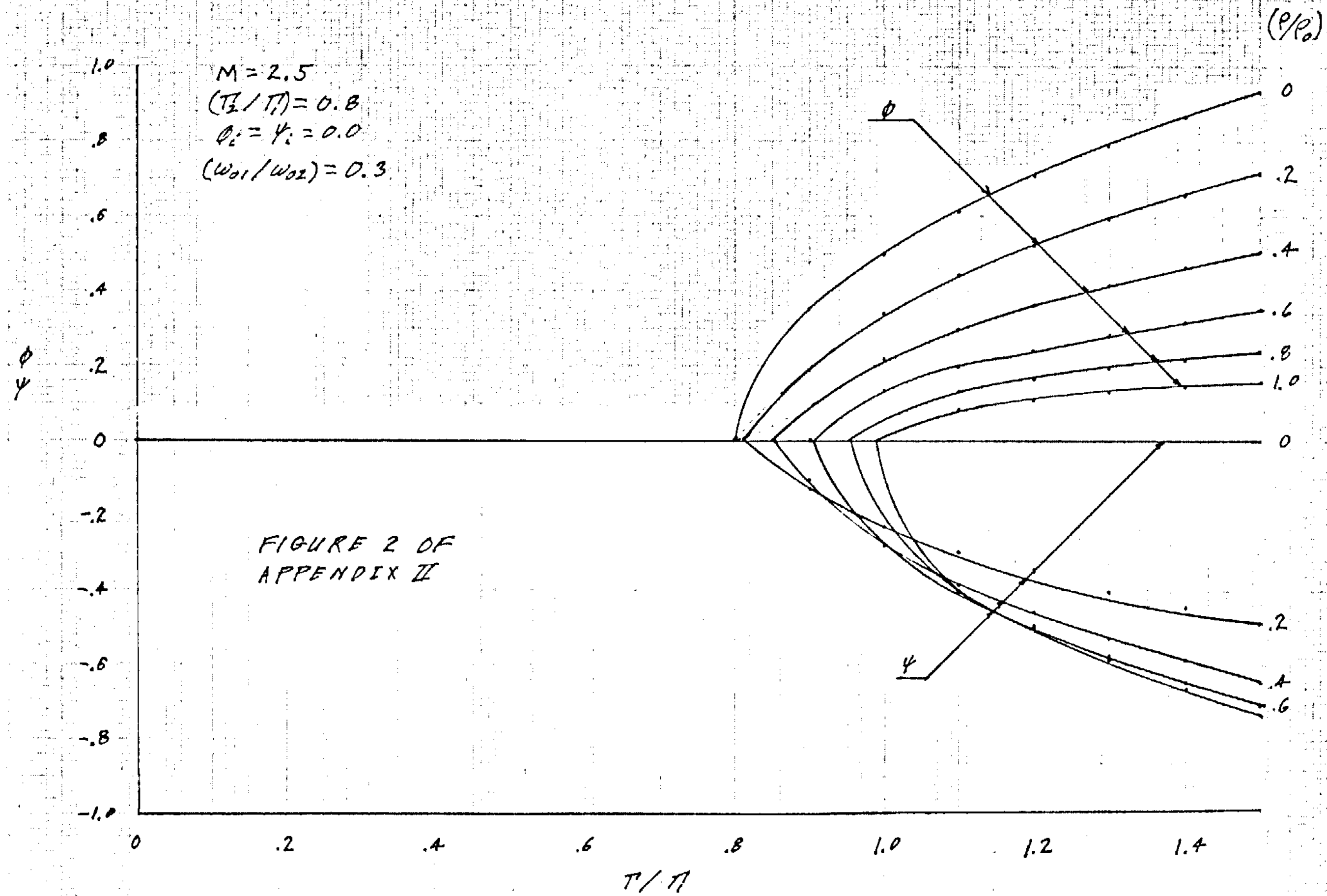

FIGURE 2 OF
APPENDIX II

FIGURE 3 OF
APPENDIX II

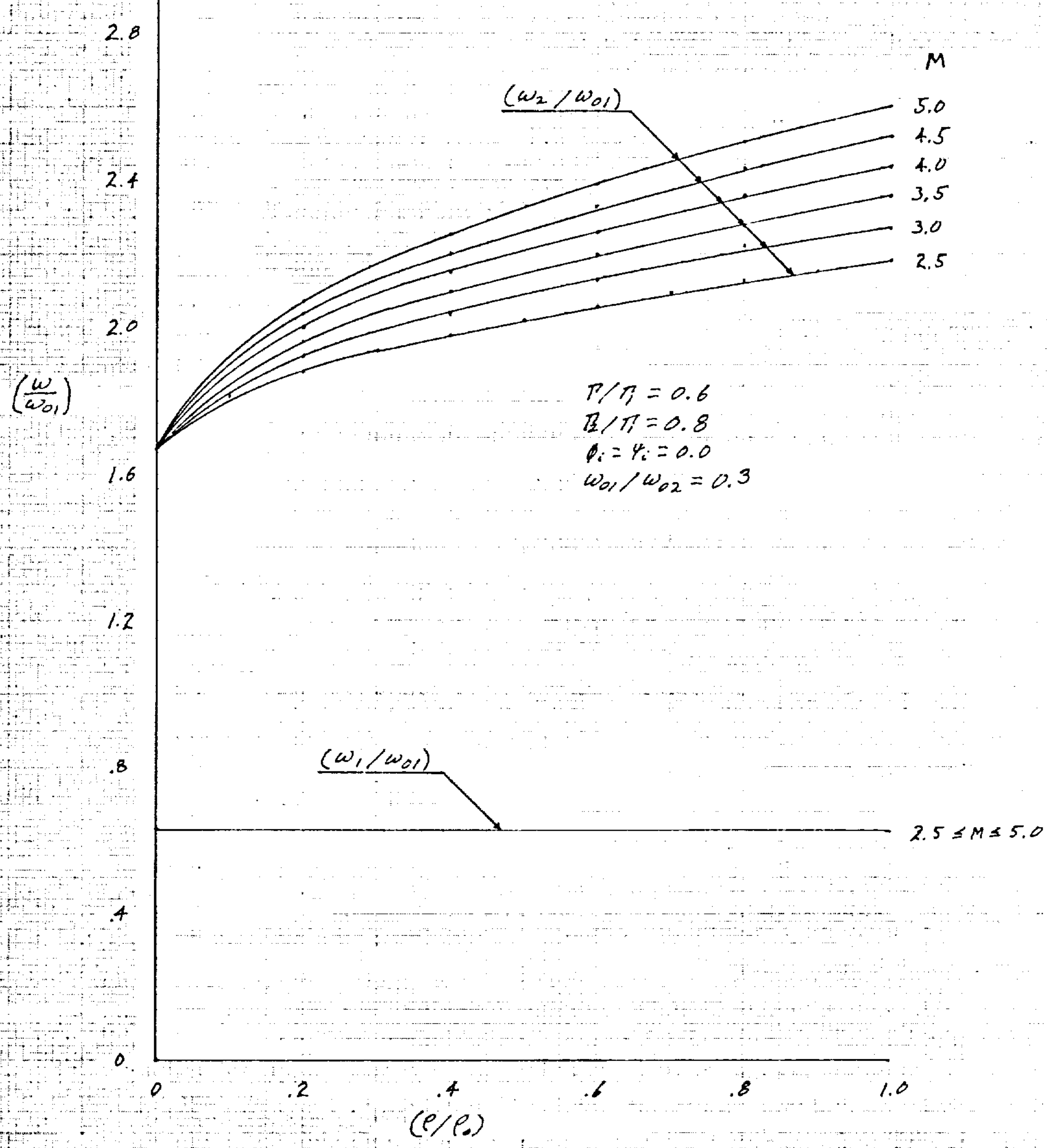

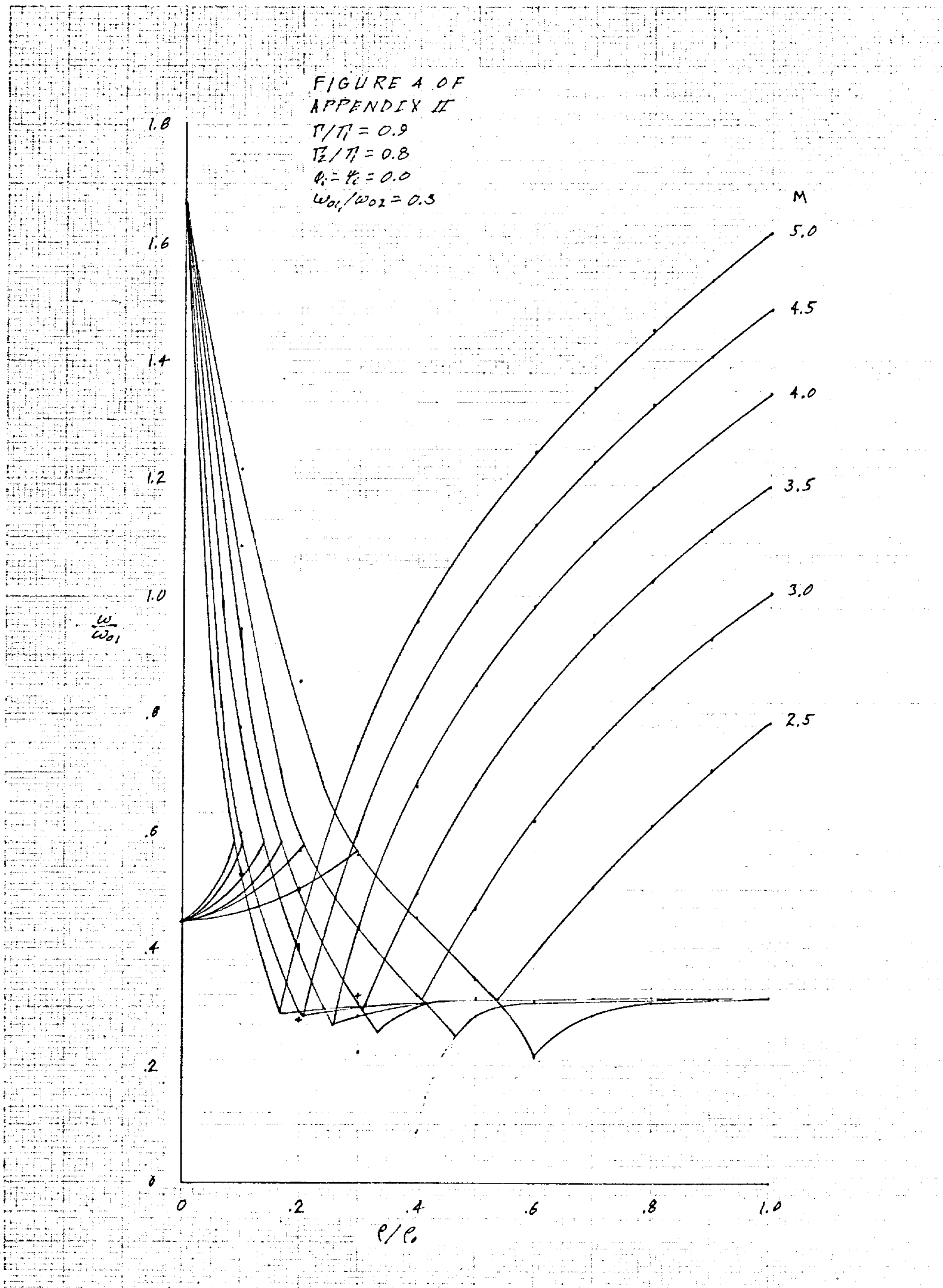

FORM 351-F-4 REV 10/67

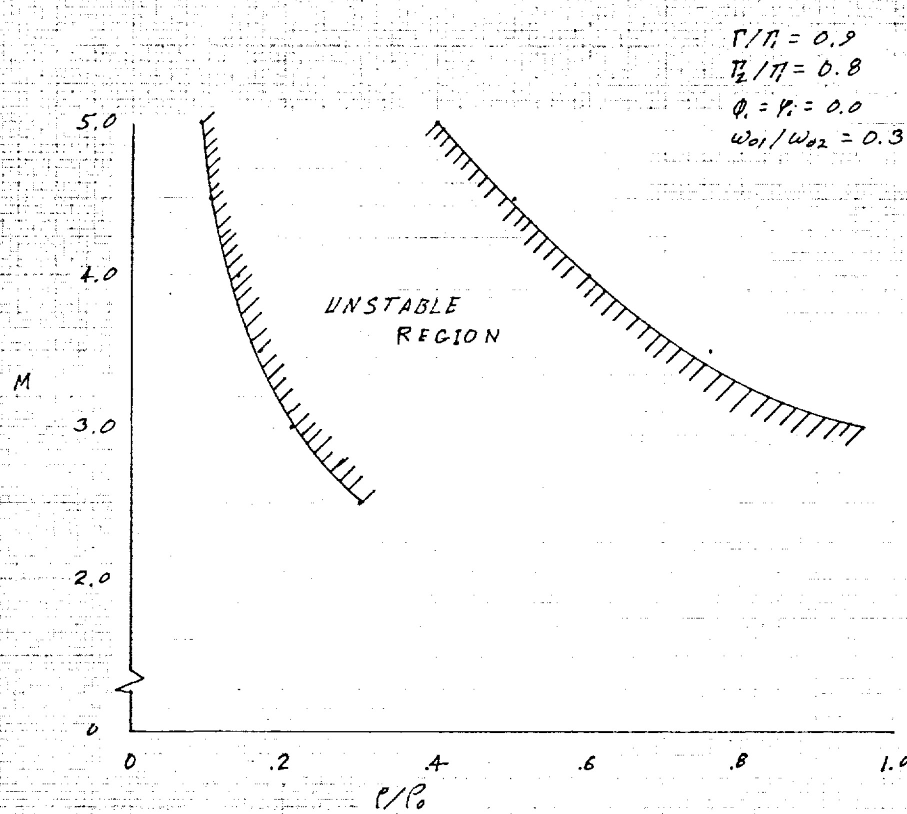

FIGURE 5 OF APPENDIX II

FORM 351-F-4 REV 10/67

Modal Coupling in Thermally Stressed Plates*

Cecil D. Bailey

The Ohio State University, Columbus, Ohio

Abstract

An approximate, but general, solution for the frequencies, thus the effective stiffnesses, in the first and second modes of initially deformed, thermally stressed plates of any planform shape and with any boundary condition is found in terms of quantities that may be obtained from the application of linear theory. It is shown that all plates exhibit the same characteristic changes in frequency, thus stiffness, independent of planform shape, boundary conditions and temperature distribution except as these factors affect the thermal buckling eigenvalues (ΔT critical) and the natural, uniform temperature frequencies. Coupling between the modes is shown to depend upon the ratio of the thermal buckling eigenvalues and the uniform temperature frequency ratio. Analytical data are presented to show that the second mode stiffness for a plate for certain values of the parameters does not always increase in the post buckled region as implied in the literature. Experimental data, obtained from cantilever plates of different planforms, are presented to show that mode coupling is

*Supported in part by the Air Force Institute of Technology and by the Office of Aerospace Research, USAF.

readily detected and cannot be neglected if a correct prediction of the effective stiffness of a plate is desired. The analysis may readily be extended to any desired number of modes. Only a qualitative comparison is made between theory and experiment in this paper. A carefully controlled test program will be required to produce data for a quantitative comparison.

List of Symbols

B	Normal coordinate for the first mode
C	Large deflection stress function parameter
D	Plate stiffness, $Et^3/12(1-\nu^2)$
E	Modulus of elasticity
F	Large deflection stress function
G	Small deflection stress function
$I_1, \cdots, I_9$	Definite integrals involving functions W_1, W_2 and G
I_{10}	Work done by the stress over that part of the boundary on which the displacements are prescribed
T	Temperature distribution over the surface of the plate
ΔT_1	Reference temperature at which buckling in first mode occurs
ΔT_2	Reference temperature at which buckling in second mode occurs
t	Plate thickness

$\overline{U}$, $\overline{V}$	Displacement in the x and y directions respectively on that part of the boundary where the displacements are prescribed
W	Total displacement of elastic surface from the x,y plane
$\ddot{W}$	Second derivative with respect to time
W_i	Initial displacement of elastic surface from the x,y plane. Also called initial imperfection and/or initial deformation.
W_1	First mode from linear solution
W_2	Second mode from linear solution
Z	Sum of forces per unit area normal to the plane of the plate, $P(x,y,\tau) - \rho t\ddot{W}$
$P(x,y,\tau)$	Applied load over plate surface
α	Thermal coefficient of expansion
Γ	Energy due to heating or thermal loading $\iint t\alpha T(\sigma_x + \sigma_y)dxdy$
Γ_1	Value of Γ at which the perfect, unloaded plate would buckle in the first mode
Γ_2	Value of Γ at which the perfect, unloaded plate would buckle in the second mode
ε_ψ	Small amplitude dynamic displacement of first mode
ε_ϕ	Small amplitude dynamic displacement of second mode
θ	Normal coordinate for second mode

ν Poisson's ratio

ρ Density per unit volume

τ Time

ϕ Non-dimensionalized normal coordinate for second mode

ψ Non-dimensionalized normal coordinate for first mode

Φ Non-dimensional large static deflection, second mode

Ψ Non-dimensional large static deflection, first mode

ω Frequency of small amplitude vibration about large amplitude static equilibrium position

ω_{o_1} First mode, free vibration frequency, at uniform temperature

ω_{o_2} Second mode, free vibration frequency, at uniform temperature

Introduction

Heldenfels and Vosteen[2] showed that the second mode (torsional) frequency and stiffness of a thermally stressed square cantilever plate always increases after reaching some minimum value as the temperature increases. The minimum stiffness is dependent upon the initial deformation. The solution obtained is shown in Figure 1, where the parameter ϕ_i is a measure of the initial twist in the plate. They tested a square cantilever plate which had initial deformation in both the first and second modes. The plate and its initial shape are shown in Figure 2. Their plot of experimental data which verified their analytical solution is shown in Figure 3.

Breuer[4] verified the results of Heldenfels and Vosteen and extended the solution to plates of other aspect ratio.

Bailey[3] extended the analytical results of Heldenfels and Vosteen and showed that their solution for the second mode is also the solution for the first mode when the two modes are uncoupled. It can readily be shown by use of the theory of orthonormal functions that it is the solution for any uncoupled mode. However, in conducting an experimental investigation of tapered plates in the pre-buckled region, it was noted that in those instances when the heat was left on longer than usual, the second mode frequency did not increase after reaching a minimum but leveled off, indicating that the stiffening effect as recorded by others was not present. The fully tapered plate was the only exception. No attempt was made to explain the cause of this phenomena until more recent work was accomplished. That work is reported herein.

The terminology, first and second modes, is used to imply the generality of the solution to both symmetrical and unsymmetrical plates. 'Bending' and 'torsion' could be used, but these terms apply, in a strict sense, to symmetrical plates where in linear theory the symmetrical (bending) and antisymmetrical (torsion) deflections are completely uncoupled. For an unsymmetrical plate in linear theory and for all plates in non-linear theory, all modes are plate bending modes containing both symmetrical and antisymmetrical deflections.

Statement of the Problem and Basic Equations

Given an initially deformed plate of any planform shape, boundary conditions, and thickness distribution (provided the thickness distribution permits the assumption of thin plate theory), find the frequency, thus the effective stiffness, when the plate is subjected to thermal stress and large deflections. It is further assumed that the linear solutions to the small deflection problem of the perfect plate for specified boundary conditions, thickness distribution and planform shape are known. (By linear solutions is meant the small deflection solution to the vibrations problem when no thermal stresses are present, and the solution to the in-plane thermal stress problem when no displacements normal to the plane are present).

Since there is no exact solution to the differential equations of this problem, an approximate solution is obtained by using Reissner's Variational Principle[1] for large deflections:

$$\delta\left\{\iint\left[\frac{D}{2}\left\{\left[\frac{\partial^2(W-W_i)}{\partial x^2}\right]^2+\left[\frac{\partial^2(W-W_i)}{\partial y^2}\right]^2+2\nu\,\frac{\partial^2(W-W_i)}{\partial x^2}\,\frac{\partial^2(W-W_i)}{\partial y^2}\right.\right.\right.$$

$$\left.+\,2(1-\nu)\left[\frac{\partial^2(W-W_i)}{\partial x\partial y}\right]^2\right\}+\frac{t}{2}\left\{\frac{\partial^2 F}{\partial x^2}\left[\left(\frac{\partial W}{\partial y}\right)^2-\left(\frac{\partial W_i}{\partial y}\right)^2\right]\right.$$

$$\left.+\,\frac{\partial^2 F}{\partial y^2}\left[\left(\frac{\partial W}{\partial x}\right)^2-\left(\frac{\partial W_i}{\partial x}\right)^2\right]-2\,\frac{\partial^2 F}{\partial x\partial y}\left[\frac{\partial W}{\partial x}\,\frac{\partial W}{\partial y}-\frac{\partial W_i}{\partial x}\,\frac{\partial W_i}{\partial y}\right]\right\}$$

$$-\,\frac{t}{2E}\left\{\left(\frac{\partial^2 F}{\partial x^2}\right)^2+\left(\frac{\partial^2 F}{\partial y^2}\right)^2-2\nu\,\frac{\partial^2 F}{\partial x^2}\,\frac{\partial^2 F}{\partial y^2}+2(1-\nu)\left(\frac{\partial^2 F}{\partial x\partial y}\right)^2\right\}$$

$$\left.-\,t\alpha\,T(x,y,\tau)\left[\frac{\partial^2 F}{\partial x^2}+\frac{\partial^2 F}{\partial y^2}\right]\right]dxdy-\iint[P(x,y,\tau)-\rho t\,\ddot{W}]W\,dxdy$$

$$\left.+\int_c\left[\frac{\partial^2 F}{\partial y^2}\,\overline{U}+\frac{\partial^2 F}{\partial x^2}\,\overline{V}\right]ds\right\}=0$$

In the application of this minimal energy principle the generality of the large deflection solution obtained is a result of the orthonormal functions chosen for the deflection function. Two functions must be assumed: the deflection function, W, and the stress function, F.

The deflection function is assumed to be,

$$W(x,y,\tau) = B(\tau)W_1(x,y) + \theta(\tau)W_2(x,y)$$

where $W_1(x,y)$ and $W_2(x,y)$ are the first and second buckling or vibration modes, as determined from the linear solution of whatever plate problem happens to be prescribed. Thus, these functions are orthogonal and satisfy the plate displacement boundary conditions. B and θ are undetermined parameters, in this case normal coordinates, for the modes W_1 and W_2. Although it is arbitrary, W_i, the initial displacement, is taken to be the same functional form as the large deflection mode,

$$W_i(x,y) = B_i \; W_1(x,y) + \theta_i \; W_2(x,y)$$

B_i and θ_i are the measured amplitudes that define the magnitude of the initial displacement.

The stress function for large deflections is assumed to be

$$F = C(\tau) \; G(x,y)$$

where $G(x,y)$ is the stress function obtained from a linear solution of the stress distribution; thus, it satisfies the stress boundary conditions for whatever planform shape the plate may have. C, B, and θ are undetermined parameters that must be found from the application of Reissner's variational principle.

Substitution of the assumed functions into the variational equation yields three equations in the three unknowns:

$$\ddot{B} + \frac{I_2}{I_1}(B-B_i) + C\,\frac{I_3}{I_1}\,B = \frac{I_4}{I_1} \qquad (1)$$

$$\ddot{\theta} + \frac{I_6}{I_5}(\theta - \theta_i) + C\,\frac{I_7}{I_5}\theta = \frac{I_8}{I_5} \tag{2}$$

$$C = \frac{I_3}{I_9}(B^2 - B_i^2) + \frac{I_7}{I_9}(\theta^2 - \theta_i^2) - \frac{\Gamma}{I_9} - \frac{I_{10}}{I_9} \tag{3}$$

where, the I_i, $i = 1, \cdots, 9$, are numbers obtained from evaluation of definite integrals in the linear solution. These integrals are given in Appendix I. I_{10} is known from the prescribed boundary conditions and is taken to be zero in this paper.

Substitution of the third equation into the first two yields two equations from which B and θ may be determined. From these equations it may be noted that no coupling exists unless large deflections are present.

$$\ddot{B} + B\frac{I_2}{I_1}\left[1 - \frac{I_3}{I_2 I_9}\Gamma - \frac{I_3^2}{I_2 I_9}B_i^2 + \frac{I_3 I_7}{I_2 I_9}(\theta^2 - \theta_i^2) - \frac{I_3 I_{10}}{I_2 I_9}\right] + \frac{I_3^2}{I_1 I_9}B^3 = \frac{I_4}{I_1} + \frac{I_2}{I_1}B_i \quad , \tag{4}$$

$$\ddot{\theta} + \theta\frac{I_6}{I_5}\left[1 - \frac{I_7}{I_6 I_9}\Gamma - \frac{I_7^2}{I_6 I_9}\theta_i^2 + \frac{I_3 I_7}{I_6 I_9}(B^2 - B_i^2) - \frac{I_7 I_{10}}{I_6 I_9}\right] + \frac{I_7^2}{I_5 I_9}\theta^3 = \frac{I_8}{I_5} + \frac{I_6}{I_5}\theta_i \tag{5}$$

As a result of the choice of assumed functions, an examination of the linear equations will show that for $I_{10} = 0$ (Reference 2, 3, or 4):

$$\frac{I_2}{I_1} = \omega_{o_1}^2$$, the first mode, uniform temperature free vibration frequency.

$$\frac{I_2 I_9}{I_3} = \Gamma_{1\,critical}$$, the first mode, uncoupled, unloaded, perfect plate thermal buckling parameter for the prescribed temperature distribution.

$$\frac{I_4}{I_2} = B_o$$, the first mode deflection under any applied load normal to the plate surface.

$$\frac{I_6}{I_5} = \omega_{o_2}^2$$, the second mode, uniform temperature free vibration frequency.

$$\frac{I_6 I_9}{I_7} = \Gamma_{2\,critical}$$, the second mode, uncoupled, unloaded, perfect plate thermal buckling parameter for the prescribed temperature distribution.

$$\frac{I_8}{I_6} = \theta_o$$, the second mode deflection under the applied load normal to the plate surface.

Now divide equations (4) and (5) by I_2/I_1 and I_6/I_5 respectively, make the foregoing substitutions followed by the following coordinate transformations:

$$\psi^2 = \frac{I_3}{\Gamma_1} B^2 \quad ,$$

$$\phi^2 = \frac{I_7}{\Gamma_2} \theta^2 \quad .$$

The resulting equations are:

$$\frac{\ddot{\psi}}{\omega_{o_1}^2} + \psi\left[1 - \frac{\Gamma}{\Gamma_1} - \psi_i^2 + \frac{\Gamma_2}{\Gamma_1}(\phi^2 - \phi_i^2) - \frac{I_{10}}{\Gamma_1 \cancel{\omega_{o_1}^2 I_7}}\right] + \psi^3 = \psi_o + \psi_i \quad , \qquad (6)$$

$$\frac{\ddot{\phi}}{\omega_{o_2}^2} + \phi\left[1 - \frac{\Gamma}{\Gamma_2} - \phi_i^2 + \frac{\Gamma_1}{\Gamma_2}(\psi^2 - \psi_i^2) - \frac{I_{10}}{\Gamma_2 \cancel{\omega_{o_2}^2 I_9}}\right] + \phi^3 = \phi_o + \phi_i \quad . \qquad (7)$$

When the displacements over that part of the boundary where the displacements are prescribed are zero, the integral $I_{10} = 0$. Other wise, it is seen that prescribing boundary displacements will cause the same trend of stiffening as prescribing Γ, ψ_i, or ϕ_i.

It is possible that I_4, I_8, and I_{10} as well as Γ may, any one or all, be functions of time, in which case the problem would be a large amplitude vibration problem under, at most, four different forcing functions.

The assumption is now made that I_4, I_8, and I_{10} are not functions of time and that the rate of change of the displacements as a result of the rate of change of Γ with time is sufficiently slow that the deflections caused by temperature may be treated as a statics problem. Thus, under heat input in the plane of the plate and load normal to the plane, the plate may undergo large static deflections about which small amplitude dynamic oscillations may occur. The square of the frequency of these oscillations is a direct measure of the effective stiffness in the mode and at the displacement under investigation.

To find the frequency of the small amplitude oscillations (see Appendix II) let,

$$\psi = \varepsilon_{\psi} + \Psi$$

$$\phi = \varepsilon_{\phi} + \Phi$$

Substitution of these quantities into equations (6) and (7) produces two equations for the frequencies when $(\omega_{o_1}/\omega_{o_2})^2 << 1$,

$$\left(\frac{\omega}{\omega_o}\right)_1^2 = 1 - \frac{\Gamma}{\Gamma_1} + 3\Psi^2 - \psi_i^2 + \frac{\Gamma_2}{\Gamma_1}(\Phi^2 - \phi_i^2) - \frac{I_{10}}{\cancel{\omega_{o_1}^2 I_9}\,\Gamma_1} \tag{8}$$

$$\left(\frac{\omega}{\omega_o}\right)_2^2 = 1 - \frac{\Gamma}{\Gamma_2} + 3\Phi^2 - \phi_i^2 + \frac{\Gamma_1}{\Gamma_2}(\Psi^2 - \psi_i^2) - \frac{I_{10}}{\cancel{\omega_{o_2}^2 I_9}\,\Gamma_2} \tag{9}$$

Since ψ_i, ϕ_i, Γ, and I_{10} are specified quantities, it is only necessary to find Φ and Ψ in order to calculate the frequencies. Setting the inertial terms equal to zero in equations (6) and (7) yields the static deflection equations,

$$\Psi^3 + \Psi\left[1 - \frac{\Gamma}{\Gamma_1} - \psi_i^2 + \frac{\Gamma_2}{\Gamma_1}(\Phi^2 - \phi_i^2) - \frac{I_{10}}{\Gamma_1\,\cancel{\omega_{o_1}^2 I_9}}\right] = \psi_o + \psi_i \tag{10}$$

$$\Phi^3 + \Phi\left[1 - \frac{\Gamma}{\Gamma_2} - \phi_i^2 + \frac{\Gamma_1}{\Gamma_2}(\Psi^2 - \psi_i^2) - \frac{I_{10}}{\Gamma_2\,\cancel{\omega_{o_2}^2 I_9}}\right] = \phi_o + \phi_i \tag{11}$$

Therefore, the problem reduces to that of finding Φ and Ψ from the above two equations and then substituting these results into equations (8) and (9) to get the effects on frequency and stiffness. Note that the ratio of the thermal buckling eigenvalues,

Γ_2/Γ_1 (or, $\Delta T_2/\Delta T_1$, see Appendix III) determines the degree of coupling for the large amplitude, static deflections. Both the thermal buckling eigenvalue ratio and the uniform temperature frequency ratio, $\omega_{o_1}/\omega_{o_2}$, influence the degree of coupling in the frequency equations. In equations (8) and (9) the frequency ratio, $\omega_{o_1}/\omega_{o_2}$, has been assumed small, thus its influence on the coupling has been omitted. A parametric study has been made of equations (8), (9), (10) and (11) for values of thermal loading ratio, Γ/Γ_2, from 0 to 2.0 and for various combinations of the parameters, $\Gamma_1/\Gamma_2 = \Delta T_1/\Delta T_2$, ϕ_i, and ψ_i, with $I_{10} = 0$.

It was found from the parametric study that for $\Delta T_1/\Delta T_2$ sufficiently greater than unity, the second mode frequency always increases after reaching a minimum as predicted in Reference 2. However, it was also found that the first frequency levels off after reaching a minimum regardless of the magnitude of the initial deflections, ψ_i and ϕ_i. But it was also found that for $\Delta T_1/\Delta T_2$ sufficiently less than unity, the first mode frequency always increases after reaching a minimum while the second mode levels off at a minimum, again independent of the magnitude of the initial deflections.

The interesting results occur when $\Delta T_1/\Delta T_2$ is sufficiently close to unity. For $\Delta T_1/\Delta T_2 = 1$ the relative magnitude of the initial displacement parameters control which mode increases and which levels off, although it is possible that both may increase.

For $\Delta T_1/\Delta T_2$ sufficiently close to unity, the ratio of $\Delta T_1/\Delta T_2$ combined with ψ_i and ϕ_i determines the frequency response. The effect of ω_{o1}/ω_{o2} remains to be investigated.

A qualitative comparison of parametric study results with experimental frequency data for $\Delta T_1/\Delta T_2$ in the neighborhood of unity is shown in the following figures.

The experimental data recorded at the Air Force Institute of Technology are shown in Figures 4, 5, 7, and 8. ψ_i and ϕ_i are not known, but the ratio $\Delta T_1/\Delta T_2$ for the rectangular plate, Fig. 4, was calculated as 1.029. Note that the first mode frequency increases while the second mode frequency levels off. Figure 5 shows the same phenomena for a slightly tapered plate.

Figure 6 shows the parametric response for the coupled first and second modes of a plate for which,

$$\frac{\Delta T_1}{\Delta T_2} = 1.0, \ \phi_i = 0.02, \ \psi_i = 0.1$$

$$\psi_o = \phi_o = I_{10} = 0, \ (\omega_{o1}/\omega_{o2})^2 << 1$$

The first mode frequency increases after buckling while the second mode levels off, just as in the experiment.

Figure 7 and Fig. 8 show the experimental results for highly tapered plates of the same aspect ratio and thickness as the previous plates. The calculated values of $\Delta T_1/\Delta T_2 > 1.1$ are shown in the figures. For these plates, the second mode frequency increases in the conventional manner while the first mode levels off. Again, ψ_i and ϕ_i are not known for the plates although no initial deformation was discernable by visual inspection.

Figure 9 shows that for $\Delta T_1/\Delta T_2$ = 1.1, the analytical response has the same trend as the experimental data when the initial imperfections are very small. It should be noted that the initial slope of the frequency response curves is affected by the initial deflection. Therefore, extrapolation of experimental data to obtain ΔT_1 and ΔT_2 may lead to erroneous results.

A comparison of theoretical to experimental results from Reference 2 is shown in Figure 3. The theoretical curve does not contain any effect of initial deformation in the bending mode, although the initial plate shape, Figure 2, indicates quite large bending and camber. Thus, the effect of finite ψ_i is present in the experimental data.

Figure 10 shows two curves for $\Delta T_1/\Delta T_2$ = 1.1. The dashed curve is for ϕ_i = 0.06 (about the correct value), and ψ_i = 0, which would be representative of the analytical curve in Figure 3. The solid curve in Figure 10 occurs when ψ_i = 0.2 and would be representative of the experimental curve in Figure 3 which may explain in part the disagreement between experiment and theory in Reference 2.

Conclusions

Both experimental and analytical data indicates strong coupling between the first two modes of plates with in-plane stresses. The onset of significant coupling varies with the initial imperfections and with the ratio of in-plane buckling parameters, $\Delta T_1/\Delta T_2$.

For $\omega_{o_1}/\omega_{o_2}$ sufficiently small, the post buckling behavior of plates for which $\Delta T_1/\Delta T_2 \neq 1$, is determined by the ratio $\Delta T_1/\Delta T_2$. If $\Delta T_1/\Delta T_2$ is sufficiently less than 1, the second mode frequency will always level off and the first mode frequency will increase, whereas for $\Delta T_1/\Delta T_2$ sufficiently greater than 1, the first mode will level off and the second mode will increase. For $\Delta T_1/\Delta T_2$ sufficiently close to 1, the relative magnitudes of the initial imperfections will determine which mode levels off and which mode increases.

Equations (8), (9), (10), and (11) and Appendix II shows that the small amplitude vibration frequency about the large amplitude static equilibrium position is independent of planform shape, boundary conditions, thickness distribution and temperature distribution except as these factors affect the thermal buckling parameters and the uniform temperature frequencies.

The influence of $\omega_{o_1}/\omega_{o_2}$ remains to be determined. Experimental data for quantitative comparison of theory with experiment needs to be obtained including a more careful quantitative evaluation of arbitrary initial imperfection than is given in Reference 2. Further, the essentially second order purturbation on the linear theory presented herein should be evaluated as to its range of validity by comparison to experimental data obtained under carefully controlled conditions.

Appendix I

The I_i are nine integrals of known functions over the plate surface and are known quantities from the linear solution.

$$I_1 = \iint \rho t W_1^2 \, dxdy$$

$$I_2 = \iint D \left\{ \left(\frac{\partial^2 W_1}{\partial x^2} \right)^2 + \left(\frac{\partial^2 W_1}{\partial y^2} \right)^2 + 2\nu \frac{\partial^2 W_1}{\partial x^2} \frac{\partial^2 W_1}{\partial y^2} + 2(1-\nu) \left(\frac{\partial^2 W_1}{\partial x \partial y} \right)^2 \right\} dxdy$$

$$I_3 = \iint t \left\{ \frac{\partial^2 G}{\partial x^2} \left(\frac{\partial W_1}{\partial y} \right)^2 + \frac{\partial^2 G}{\partial y^2} \left(\frac{\partial W_1}{\partial x} \right)^2 - \frac{\partial^2 G}{\partial x \partial y} \frac{\partial W_1}{\partial x} \frac{\partial W_1}{\partial y} \right\} dxdy$$

$$I_4 = \iint P \, W_1 \, dxdy$$

$$I_5 = \iint \rho t W_2^2 \, dxdy$$

$$I_6 = \iint D \left\{ \left(\frac{\partial^2 W_2}{\partial x^2} \right)^2 + \left(\frac{\partial^2 W_2}{\partial y^2} \right) + 2\nu \frac{\partial^2 W_2}{\partial x^2} \frac{\partial^2 W_2}{\partial y^2} + 2(1-\nu) \left(\frac{\partial^2 W_2}{\partial x \partial y} \right)^2 \right\} dxdy$$

$$I_7 = \iint t \left\{ \frac{\partial^2 G}{\partial x^2} \left(\frac{\partial W_2}{\partial y} \right)^2 + \frac{\partial^2 G}{\partial y^2} \left(\frac{\partial W_2}{\partial x} \right)^2 - 2 \frac{\partial^2 G}{\partial x \partial y} \frac{\partial W_2}{\partial x} \frac{\partial W_2}{\partial y} \right\} dxdy$$

$$I_8 = \iint P \, W_2 \, dxdy$$

$$I_9 = \iint \frac{t}{E} \left\{ \left(\frac{\partial^2 G}{\partial x^2} \right)^2 + \left(\frac{\partial^2 G}{\partial y^2} \right)^2 - 2\nu \frac{\partial^2 G}{\partial x^2} \frac{\partial^2 G}{\partial y^2} + 2(1-\nu) \left(\frac{\partial^2 G}{\partial x \partial y} \right)^2 \right\} dxdy$$

$$I_{10} = \int t \left\{ \frac{\partial^2 G}{\partial x^2} \overline{V} + \frac{\partial^2 G}{\partial y^2} \overline{U} \right\} ds$$

<u>Appendix II</u>

The equations of motion are:

$$\frac{\ddot{\psi}}{\omega_{o1}^2} + \psi^3 + \psi[1 - \frac{\Gamma}{\Gamma_1} - \psi_i^2 + \frac{\Gamma_2}{\Gamma_1}(\phi^2 - \phi_i^2) - \frac{I_{10}}{\Gamma_1 \cancel{\omega_{o1}^2 I_g}}] = \psi_o + \psi_i$$

$$\frac{\ddot{\phi}}{\omega_{o2}^2} + \phi^3 + \phi[1 - \frac{\Gamma}{\Gamma_2} - \phi_i^2 + \frac{\Gamma_1}{\Gamma_2}(\psi^2 - \psi_i^2) - \frac{I_{10}}{\Gamma_2 \cancel{\omega_{o2}^2 I_g}}] = \phi_o + \phi_i$$

Assume:

$$\psi = \varepsilon_\psi + \Psi$$

$$\phi = \varepsilon_\phi + \Phi$$

Substitute:

$$\frac{\ddot{\varepsilon}_\psi}{\omega_{o1}^2} + (\varepsilon_\psi + \Psi)^3 + [\varepsilon_\psi + \Psi][1 - \frac{\Gamma}{\Gamma_1} - \psi_i^2 + \frac{\Gamma_2}{\Gamma_1}((\varepsilon_\Phi + \Phi)^2 - \phi_i^2)$$
$$- \frac{I_{10}}{\Gamma_1 \cancel{\omega_{o1}^2 I_g}}] = \psi_o + \psi_i$$

$$\frac{\ddot{\varepsilon}_\phi}{\omega_{o2}^2} + (\varepsilon_\phi + \Phi)^3 + [\varepsilon_\phi + \Phi][1 - \frac{\Gamma}{\Gamma_2} - \phi_i^2 + \frac{\Gamma_1}{\Gamma_2}((\varepsilon_\psi + \Psi)^2 - \psi_i^2)$$
$$- \frac{I_{10}}{\Gamma_2 \cancel{\omega_{o2}^2 I_g}}] = \phi_o + \phi_i$$

Neglect all 2nd and higher order terms in ε and neglect $2\varepsilon_\psi/\Psi$ and $2\varepsilon_\phi/\Phi$ compared to unity. Subtract away the static deflection equation in each case to obtain:

$$\frac{\ddot{\varepsilon}_\psi}{\omega_{o1}^2} + [1 - \frac{\Gamma}{\Gamma_1} + 3\Psi^2 - \psi_i^2 + \frac{\Gamma_2}{\Gamma_1}(\Phi^2-\phi_i^2) - \frac{I_{10}}{\Gamma_1 \cancel{\omega_{o1}^2 I_9}}]\varepsilon_\psi + 2\,\frac{\Gamma_2}{\Gamma_1}\,\Psi\Phi\varepsilon_\phi = 0$$

$$\frac{\ddot{\varepsilon}_\phi}{\omega_{o2}^2} + [1 - \frac{\Gamma}{\Gamma_2} + 3\Phi^2 - \phi_i^2 + \frac{\Gamma_1}{\Gamma_2}(\Psi^2-\psi_i^2) - \frac{I_{10}}{\Gamma_2 \cancel{\omega_{o2}^2 I_9}}]\varepsilon_\phi + 2\,\frac{\Gamma_1}{\Gamma_2}\,\Psi\Phi\varepsilon_\psi = 0$$

Assume that the small amplitude vibration will be simple harmonic (experimental evidence supports this assumption). The result of setting the determinant of the coefficients equal to zero is the frequency equation,

$$\left(\frac{\omega^2}{\omega_{o2}^2}\right)_{1,2} = \frac{1}{2}\{C_2 + \frac{\omega_{o1}^2}{\omega_{o2}^2} C_1 \mp [(C_2 - \frac{\omega_{o1}^2}{\omega_{o2}^2} C_1) + 16\,\frac{\omega_{o1}^2}{\omega_{o2}^2}\,\Psi^2\Phi^2]^{\frac{1}{2}}\}$$

where:

$$C_1 = 1 - \frac{\Gamma}{\Gamma_1} + 3\Psi^2 - \psi_i^2 + \frac{\Gamma_2}{\Gamma_1}(\Phi^2 - \phi_i^2) - \frac{I_{10}}{\cancel{\omega_{o1}^2 I_9}\Gamma_1}$$

$$C_2 = 1 - \frac{\Gamma}{\Gamma_2} + 3\Phi^2 - \phi_i^2 + \frac{\Gamma_1}{\Gamma_2}(\Psi^2 - \psi_i^2) - \frac{I_{10}}{\cancel{\omega_{o2}^2 I_9}\Gamma_2}$$

For most practical plates the frequency of the second mode is much greater than that of the first mode. Thus, the square of the ratio, ω_{o1}/ω_{o2}, may be assumed to be much smaller than unity causing the last term in the frequency equation to become negligibly small. Note, also, that if either Ψ or Φ are zero, this term vanishes. The frequency equation then becomes,

$$\left(\frac{\omega^2}{\omega_{o2}^2}\right)_{1,2} = \frac{1}{2}\{C_2 + \frac{\omega_{o1}^2}{\omega_{o2}^2} C_1 \mp (C_2 - \frac{\omega_{o1}^2}{\omega_{o2}^2} C_1)\}$$

from which:

$$\left(\frac{\omega}{\omega_o}\right)_1^2 = \left(\frac{\omega^2}{\omega_{o_2}^2}\right)_1 \left(\frac{\omega_{o_2}}{\omega_{o_1}}\right)^2 = C_1 \tag{8}$$

$$\left(\frac{\omega}{\omega_o}\right)_2^2 = \left(\frac{\omega^2}{\omega_{o_2}^2}\right)_2^2 = C_2 \tag{9}$$

Appendix III

The thermal loading term, Γ, occurs as:

$$\Gamma = \iint \alpha t T(x,y,\tau)(\sigma_x + \sigma_y)dxdy$$

Assume that the surface temperature function $T(x,y,\tau)$ may be written relative to some reference value ΔT_{ref} or:

$$T(x,y,\tau) = \Delta T_{ref}(\tau)\ f(x,y)$$

Thus:

$$\Gamma = \Delta T_{ref} \iint \alpha t\ f(x,y)(\sigma_x + \sigma_y)dxdy$$

and

$$\Gamma_{critical} = \Delta T_{ref\ critical} \iint \alpha t\ f(x,y)(\sigma_x + \sigma_y)dxdy$$

Thus:

$$\frac{\Gamma}{\Gamma_{critical}} = \frac{\Delta T_{ref}}{\Delta T_{ref(critical)}}$$

Also:

$$\frac{\Gamma_1}{\Gamma_2} = \frac{\Delta T_{ref(critical)first\ mode}}{\Delta T_{ref(critical)second\ mode}} = \frac{\Delta T_1}{\Delta T_2}$$

References

1. Reissner, E., "On a Variational Theorem for Finite Elastic Deformations," Journal of Mathematics and Physics, Vol. XXXII, Nos. 2-3, July-October 1953, p. 129.
2. Heldenfels, R. R., and Vosteen, L. F., "Approximate Analysis of Effects of Large Deflections and Initial Twist on Torsional Stiffness of a Cantilever Plate Subjected to Thermal Stresses," NACA Report 1361, 1958, Supersedes NACA TN 4067, 1957.
3. Bailey, C. D., "Vibration and Buckling of Thermally Stressed Plates of Trapezoidal Planform," Ph.D. Dissertation, Purdue University, January 1962.
4. Breuer, D. W., "Effects of Finite Displacement, Aspect Ratio and Temperature on the Torsional Stiffness of Cantilever Plates," Proceedings of the Fourth U.S. National Congress of Applied Mechanics.

Fig. 1. Response of Uncoupled Modes, Ref. 2

Fig. 2. Initial Plate Shape, Ref. 2

Fig. 3. Frequency Response, Ref. 2

Fig. 4. Frequency Response With Coupling

Fig. 5. Frequency Response With Coupling

Fig. 6. Frequency Response With Coupling

Fig. 7. Frequency Response With Coupling

Fig. 8. Frequency Response With Coupling

Fig. 9. Frequency Response With Coupling

Fig. 10. Frequency Response With Coupling

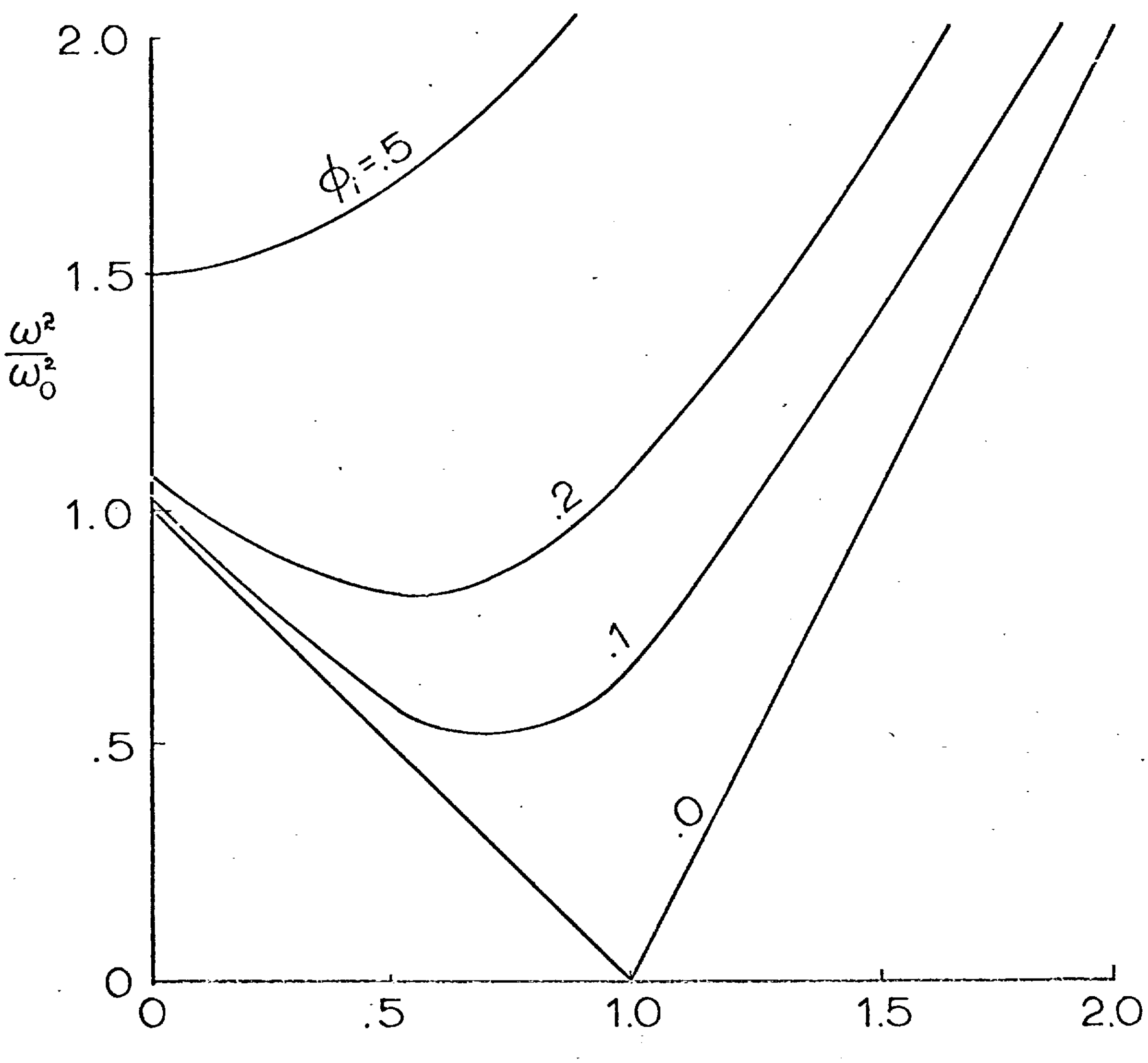

2.0
1.5
1.0
.5
0
$\frac{\omega^2}{\omega_0^2}$
$\phi_i = .5$
.2
.1
.0
0
.5
1.0
1.5
2.0
$\Delta T / \Delta T_{CR}$

Fig. 1

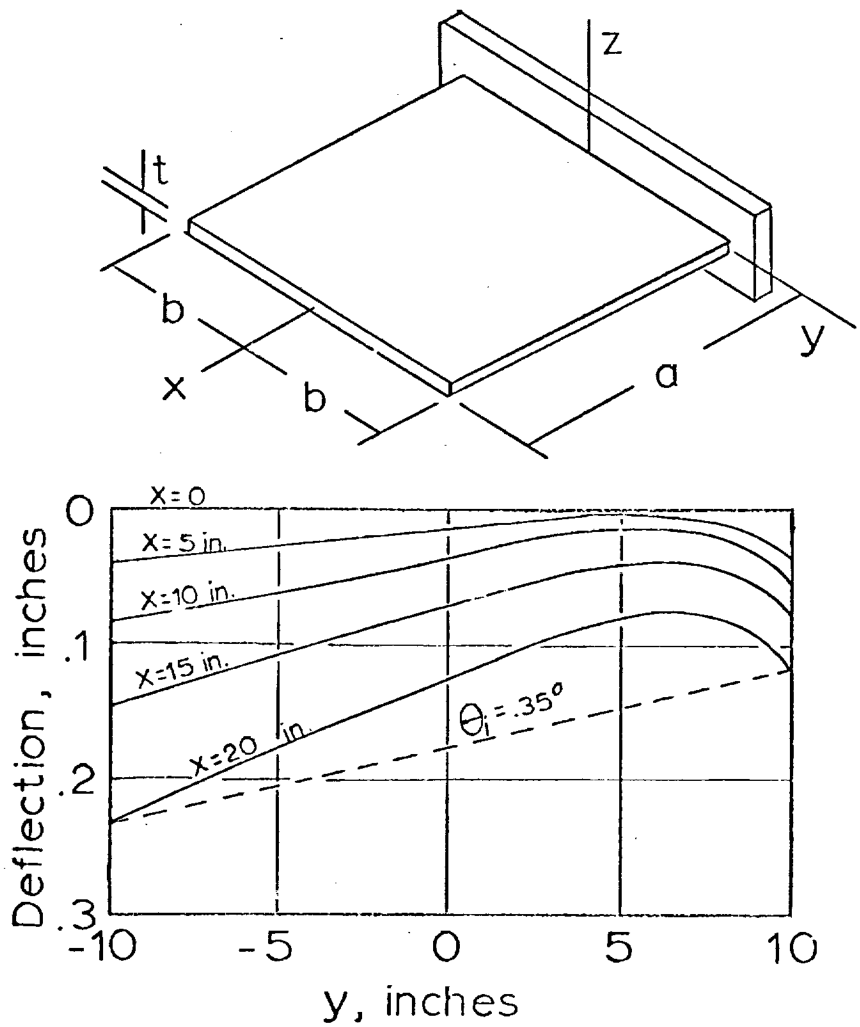

z
t
b
x
b
a
y
x=0
x=5 in.
x=10 in.
x=15 in.
x=20 in.
$\theta_i = .35^o$
Deflection, inches
0
.1
.2
.3
-10
-5
0
5
10
y, inches

FIG. 2

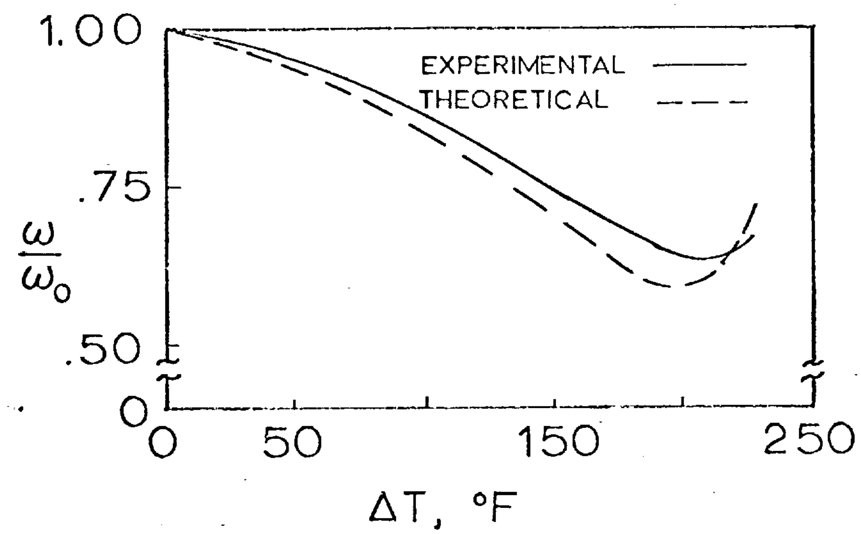
1.00
.75
.50
0
$\frac{\omega}{\omega_0}$
EXPERIMENTAL
THEORETICAL
0
50
150
250
ΔT, °F

FIG. 3

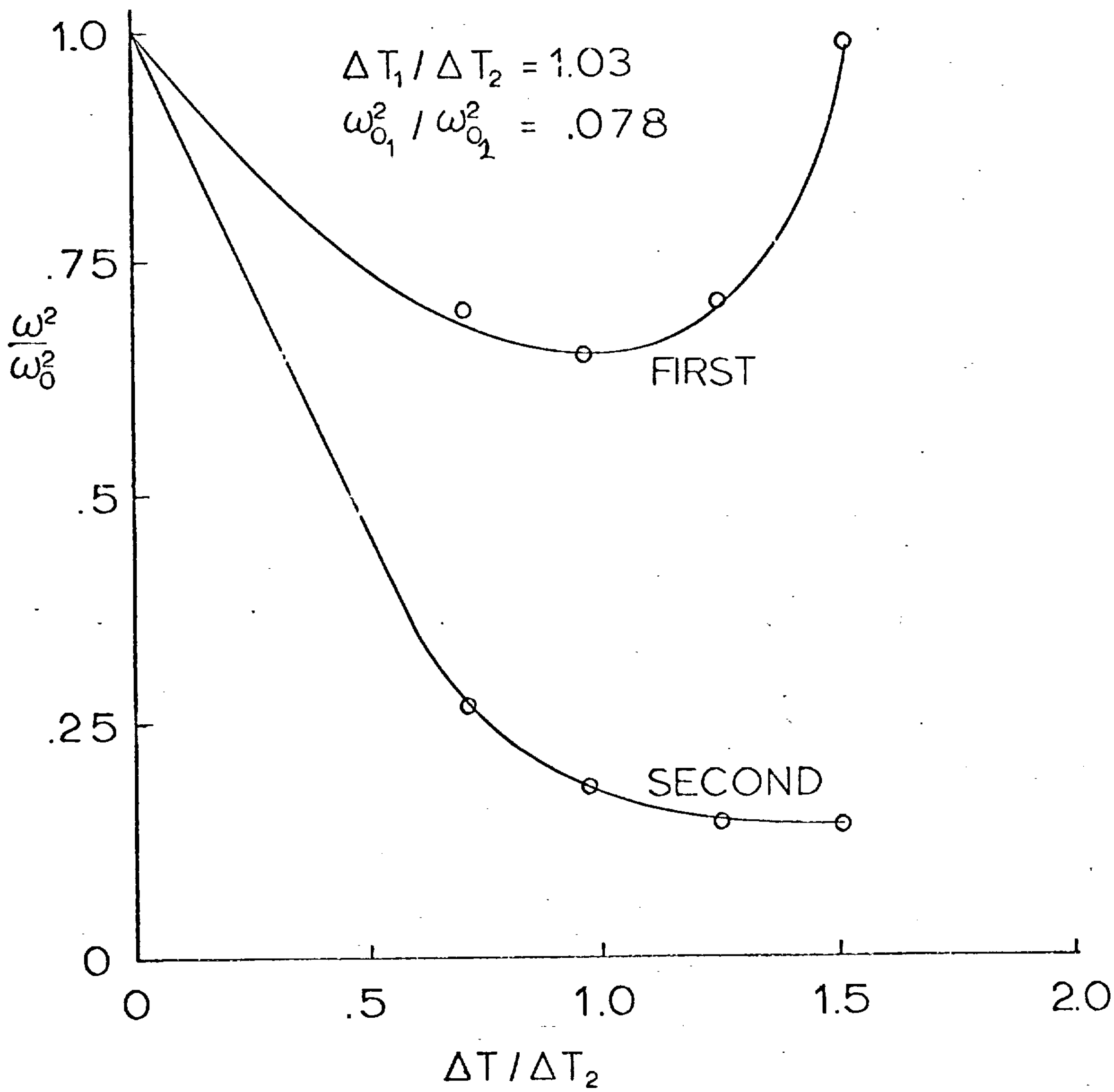

$\Delta T_1 / \Delta T_2 = 1.03$
$\omega_{0_1}^2 / \omega_{0_2}^2 = .078$
FIRST
SECOND
1.0
.75
.5
.25
0
$\frac{\omega^2}{\omega_0^2}$
0
.5
1.0
1.5
2.0
$\Delta T / \Delta T_2$

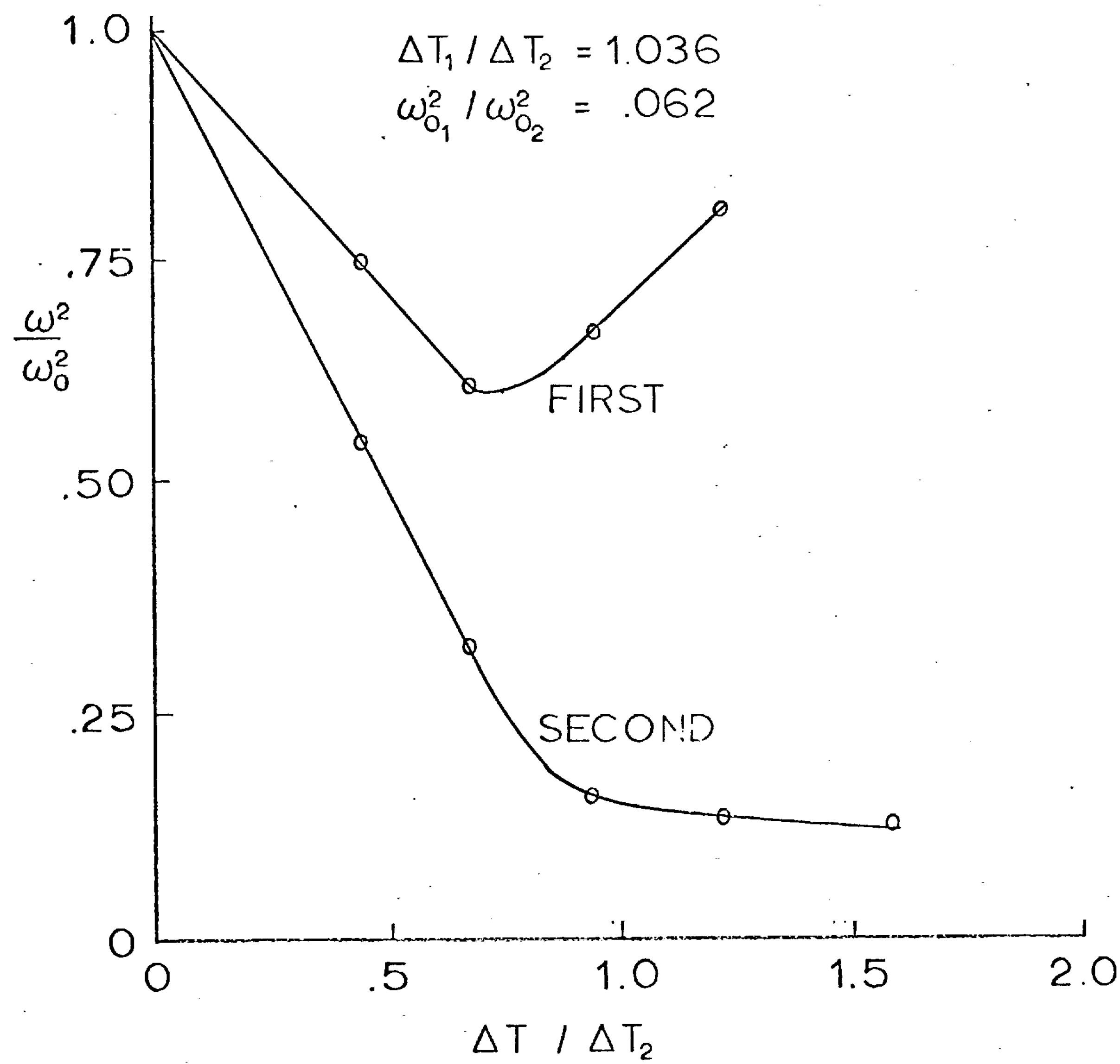
1.0
.75
.50
.25
0
$\Delta T_1 / \Delta T_2 = 1.036$
$\omega_{o_1}^2 / \omega_{o_2}^2 = .062$
$\frac{\omega^2}{\omega_o^2}$
FIRST
SECOND
0
.5
1.0
1.5
2.0
$\Delta T / \Delta T_2$

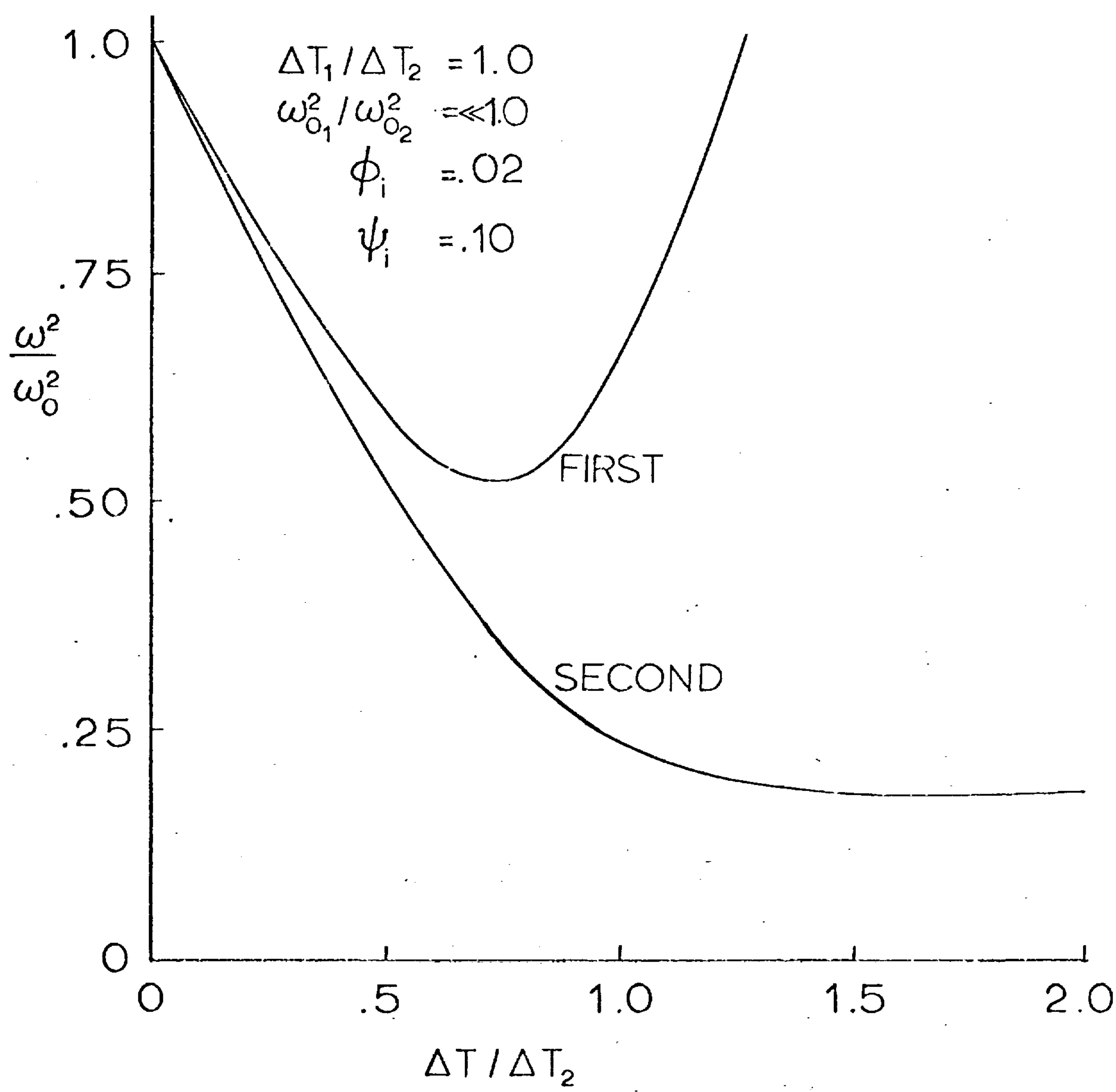
1.0
.75
.50
.25
0
$\frac{\omega^2}{\omega_0^2}$
$\Delta T_1 / \Delta T_2 = 1.0$
$\omega_{o_1}^2 / \omega_{o_2}^2 = \ll 1.0$
$\phi_i = .02$
$\psi_i = .10$
FIRST
SECOND
0
.5
1.0
1.5
2.0
$\Delta T / \Delta T_2$

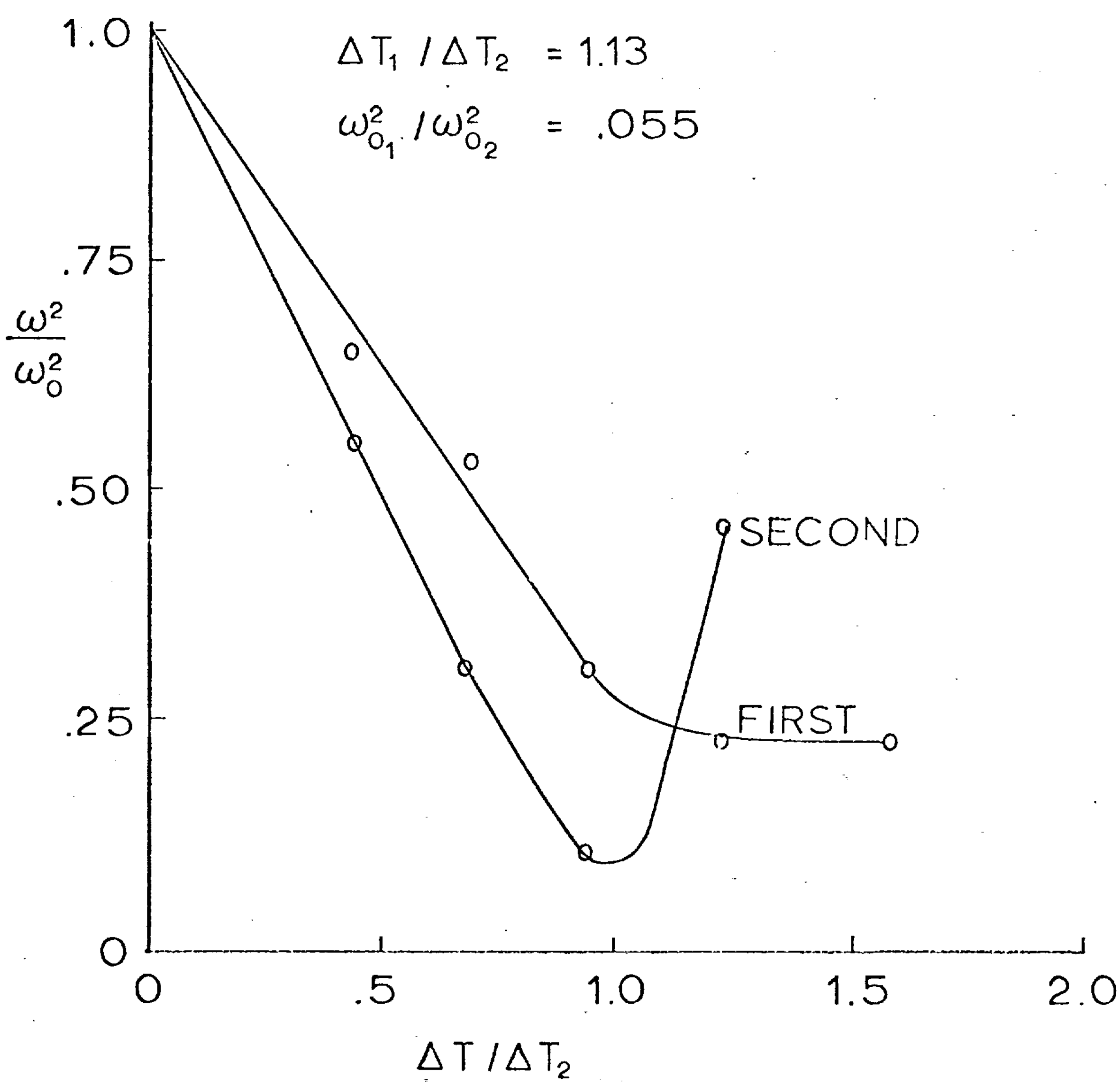

$\Delta T_1 / \Delta T_2 = 1.13$
$\omega_{o_1}^2 / \omega_{o_2}^2 = .055$
$\frac{\omega^2}{\omega_o^2}$
1.0
.75
.50
.25
0
SECOND
FIRST
0
.5
1.0
1.5
2.0
$\Delta T / \Delta T_2$

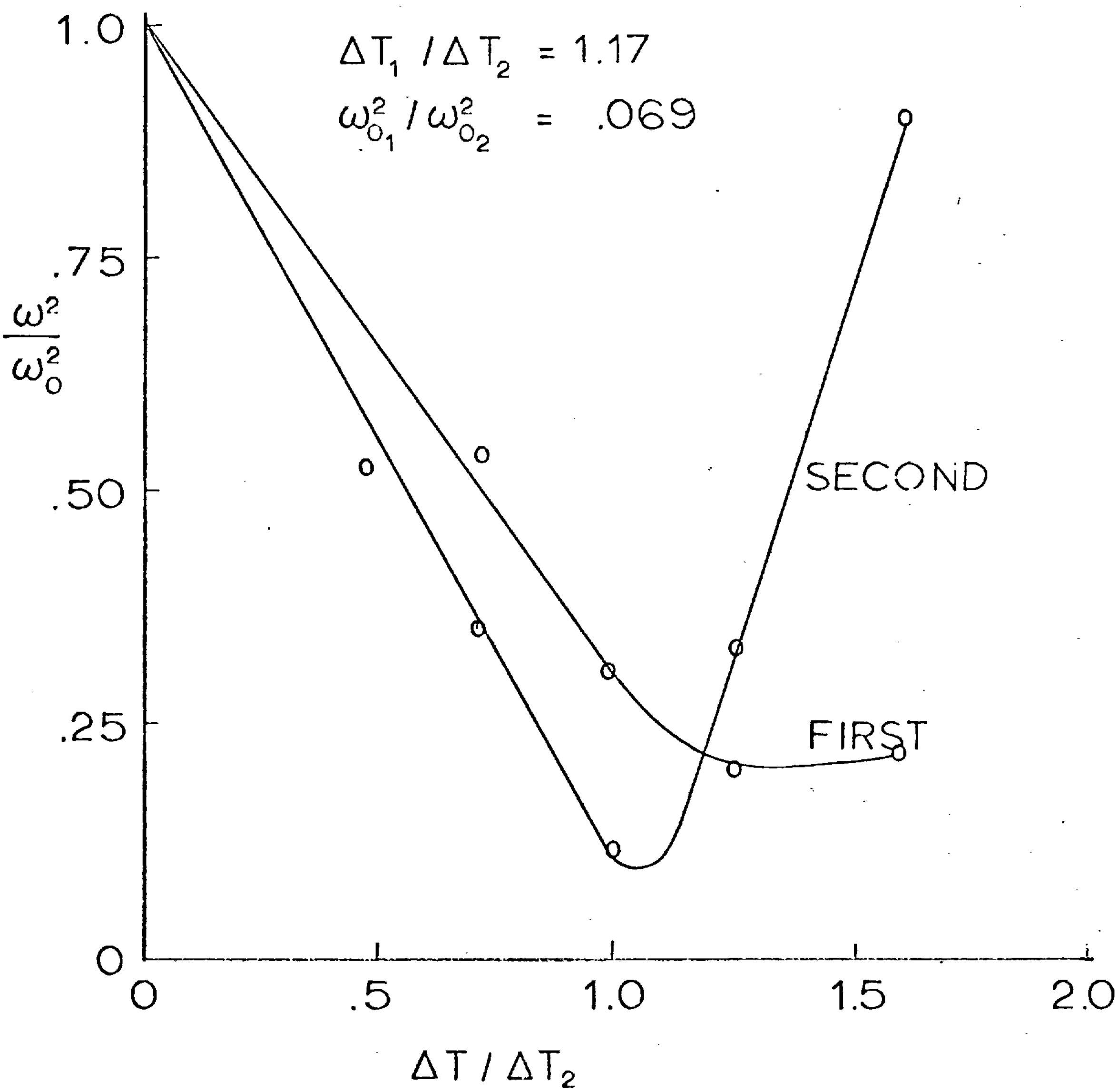
$\Delta T_1 / \Delta T_2 = 1.17$
$\omega_{0_1}^2 / \omega_{0_2}^2 = .069$
ω^2 / ω_0^2
1.0
.75
.50
.25
0
SECOND
FIRST
0
.5
1.0
1.5
2.0
$\Delta T / \Delta T_2$

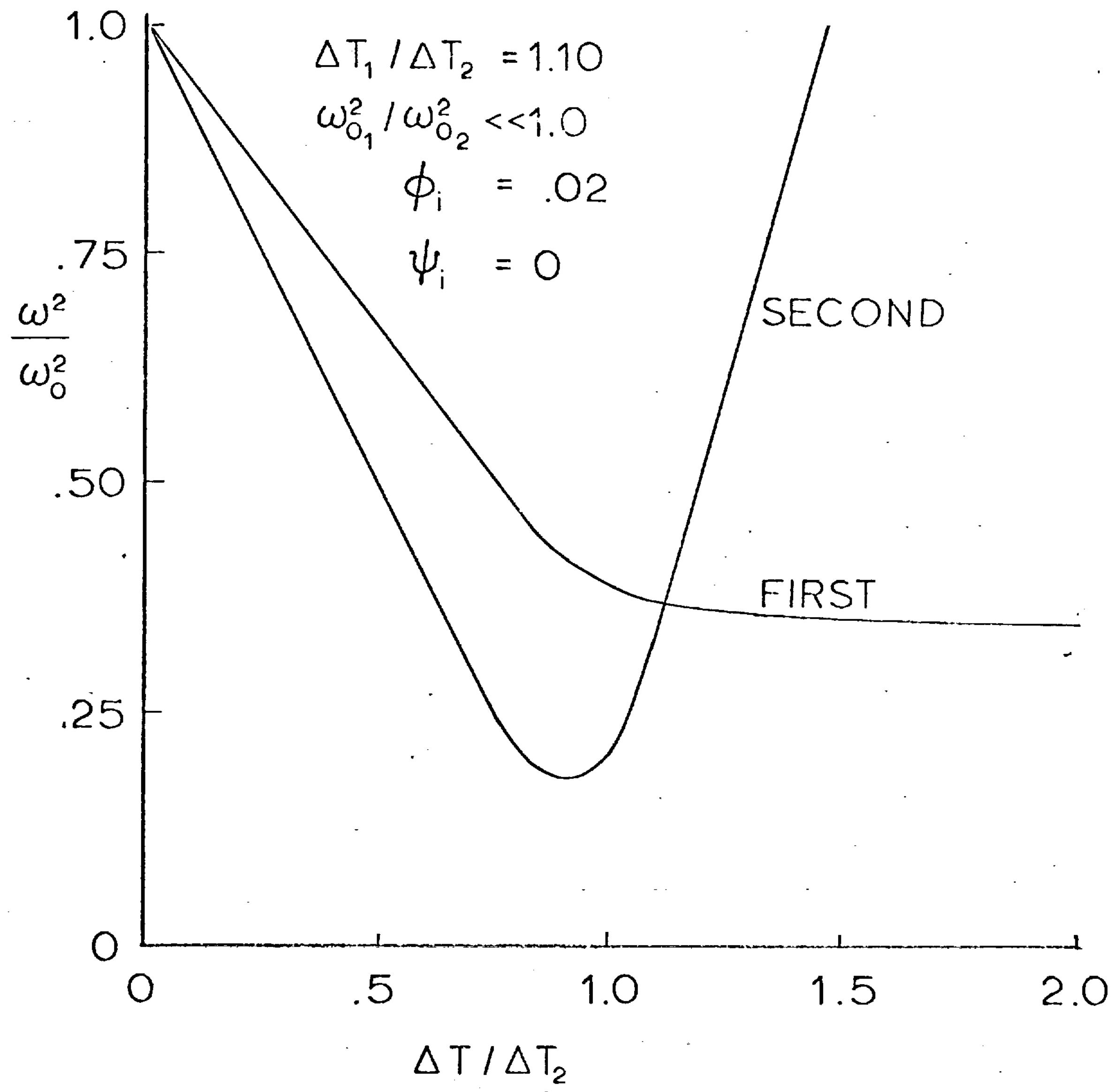

$\Delta T_1 / \Delta T_2 = 1.10$
$\omega_{0_1}^2 / \omega_{0_2}^2 << 1.0$
$\phi_i = .02$
$\psi_i = 0$
SECOND
FIRST
1.0
.75
.50
.25
0
$\frac{\omega^2}{\omega_0^2}$
0
.5
1.0
1.5
2.0
$\Delta T / \Delta T_2$

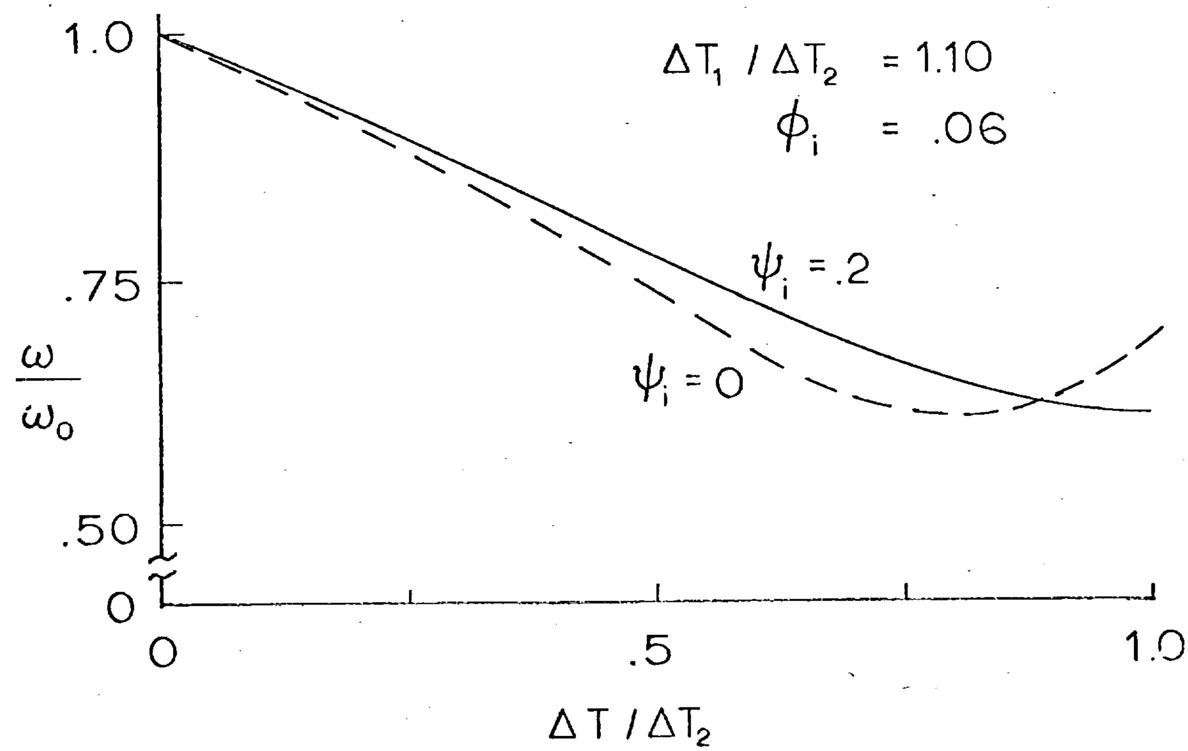

1.0
.75
.50
0
ω / ω_o
0
.5
1.0
$\Delta T / \Delta T_2$
$\Delta T_1 / \Delta T_2 = 1.10$
$\phi_i = .06$
$\psi_i = .2$
$\psi_i = 0$